

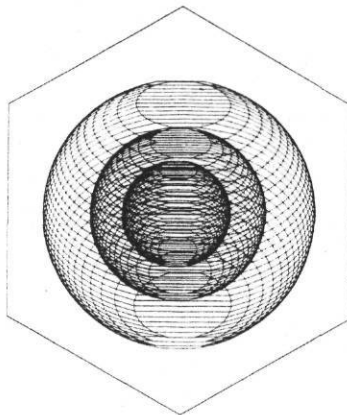
ESL-TR-89/03-01

AN EVALUATION OF THE EFFECTS OF REFRIGERANT
CHARGE ON A RESIDENTIAL CENTRAL AIR CONDITIONER
WITH ORIFICE EXPANSION

Final Report

March 1989

Dennis L. O'Neal
Chris J. Ramsey
Mohsen Farzad



**ENERGY SYSTEMS
LABORATORY**

Department of Mechanical Engineering
Texas Engineering Experiment Station
Texas A&M University
College Station, Texas 77843

AN EVALUATION OF THE EFFECTS OF REFRIGERANT
CHARGE ON A RESIDENTIAL CENTRAL AIR CONDITIONER
WITH ORIFICE EXPANSION

Final Report

March 1989

Dennis L. O'Neal
Chris J. Ramsey
Mohsen Farzad

AN EVALUATION OF THE EFFECTS OF REFRIGERANT
CHARGE ON A RESIDENTIAL CENTRAL AIR CONDITIONER
WITH ORIFICE EXPANSION

Final Report

March 1989

Dennis L. O'Neal
Chris J. Ramsey
Mohsen Farzad

Energy Systems Laboratory
Department of Mechanical Engineering
Texas A & M University

TABLE OF CONTENTS

CHAPTER		PAGE
1	INTRODUCTION	1.1
2	EXPERIMENTAL APPARATUS AND PROCEDURES	2.1
	General Description	2.1
	Psychrometric Rooms	2.1
	Testing Conditions	2.3
	Indoor Test Section	2.3
	Outdoor Test Section	2.5
	Refrigerant Side	2.6
	Data Acquisition	2.9
	Refrigerant Charging Procedures	2.11
	References	2.13
3	NOMINAL SIZE ORIFICE RESULTS	3.1
	System Performance Data	3.1
	Detailed System Data	3.10
4	RESULTS FOR ALTERNATE ORIFICES	4.1
5	COMPARISON OF THREE ORIFICES	5.1
6	CONCLUSIONS	6.1
	APPENDIX A	A.1

CHAPTER 1

INTRODUCTION

Recent studies have been conducted at Texas A & M University to quantify the effect of over/undercharging on the performance of a residential central air conditioner with two different expansion devices: capillary tubes and thermal expansion valves. A third expansion device, the short-tube orifice, is used by many manufacturers of residential air conditioners. This report summarizes the results of experiments performed for the Trane Dealer Products Group on a Trane central air conditioner which utilized short-tube orifices for flow control. The project was conducted under Trane Purchase Order No. TYR1020264-T280D.

The report is divided into 5 chapters in addition to the this chapter. Chapter 2 describes the experimental facilities and procedures used to collect and analyze data. Results are presented in Chapters 3 through 5. In all three orifices were tested. In chapter 3, data for the nominal size orifice are presented first. Data on the other two orifices are presented in Chapter 4. Comparisons between the three orifices are presented in Chapter 5. Conclusions are provided in Chapter 6.

CHAPTER 2

EXPERIMENTAL APPARATUS AND PROCEDURES

The objective of the tests was to quantify the effect of improper refrigerant charge on the performance of a Trane split system central air conditioner which used orifice expansion. Both steady state and cyclic tests were performed. The data collected included pressures and temperatures throughout the system, power consumption, capacity, EER, SEER, and refrigerant and air flow rates. The experimental apparatus used in these tests was the similar to one used in previous tests[1]. It allowed for the measurement of all important performance parameters. The air conditioner testing apparatus and testing procedure are described below.

General Description

The test apparatus was located in the psychrometric rooms of the Energy Systems Laboratory at the Texas A & M University Research Annex. The general layout of the test apparatus is given in Figure 2.1. The psychrometric rooms simulated the indoor and outdoor conditions (temperature and humidity) necessary for air conditioner performance testing.

The indoor test section consisted of the indoor coil (evaporator) and the indoor air flow chamber. Conditioned air from the indoor room was drawn through the indoor test section by the air flow chamber fan. The air flowed through the test section. A damper was mounted on the outlet that was adjustable and was set to maintain a constant air flow of 1200 cubic feet per minute(cfm) through the indoor test coil. The air was routed back into the indoor room after leaving the chamber.

The outdoor room test section consisted of the compressor and outdoor coil. The conditioned outdoor air entered the outdoor coil and was exhausted by the unit fan back into the room through the outdoor coil.

Psychrometric Rooms

The psychrometric rooms could simulate all testing conditions required for air conditioning and heat pump performance testing. Dew point and room temperatures can be maintained within +/-0.2 F of the set point. The room temperature was controlled by a Texas Instruments TI-550 controller which was integrated into the control system of the rooms.

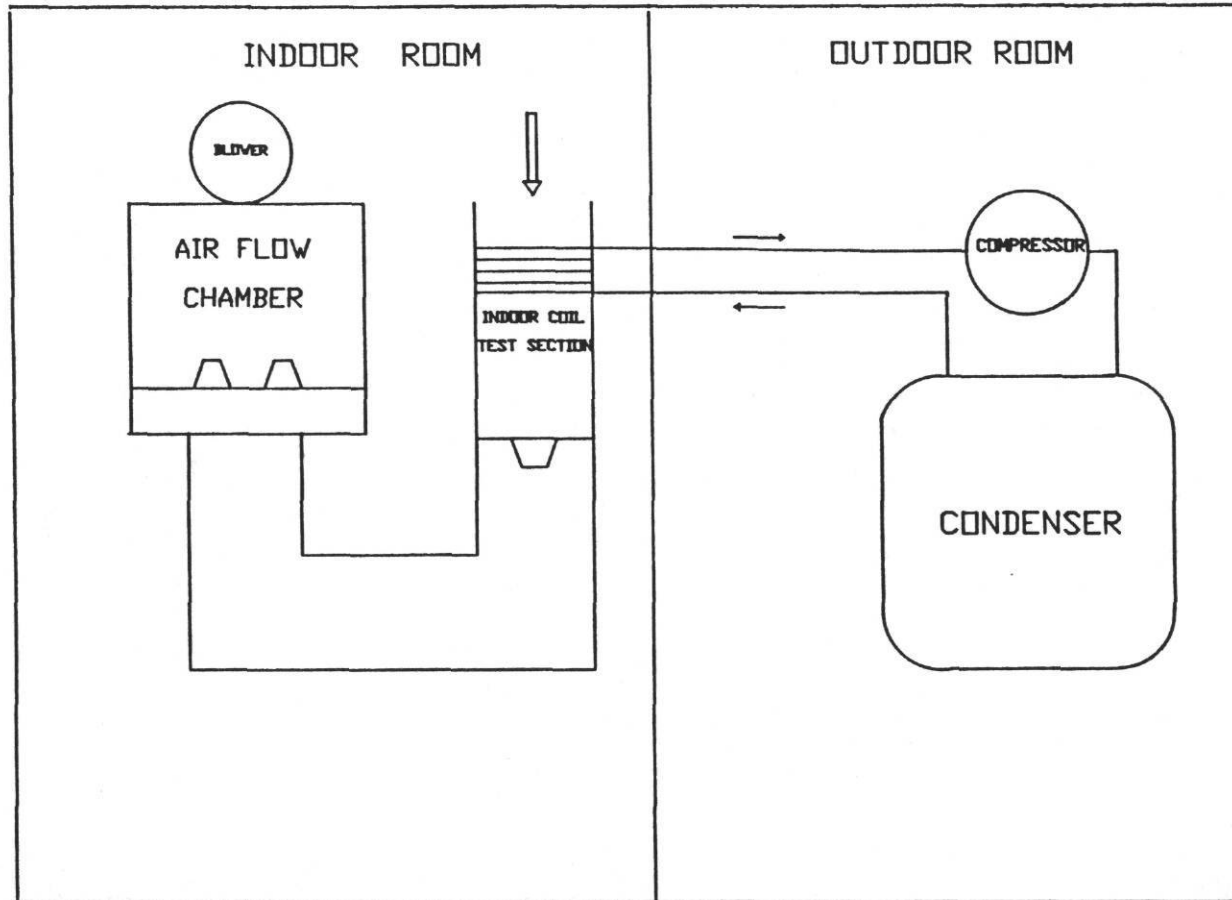


Figure 2.1 - General layout of the air conditioner in the psychrometric rooms.

Room temperatures were maintained with chilled water coils and electric resistance heaters. The chilled water coils were fed with an ethylene glycol solution that was chilled by a 105 ton capacity chiller. A 300 gallon chilled water thermal storage tank was mounted in the chilled water system to stabilize chilled water temperature. There were four banks of electric heaters in each room with 9900 watts per bank.

Humidity levels in the rooms were controlled by electric humidifiers, a dehumidification coil, and a desiccant dehumidifier. The dehumidification coils were fed from the same circuit as the cooling coils. The humidifiers were mounted in each room and supplied steam directly into the supply air duct. The desiccant dehumidifier was used to dry the indoor air for tests requiring low humidity.

Testing Conditions

The testing conditions used for the steady state wet and dry coils and cyclic tests were those prescribed by the Department of Energy (DOE) and the Air Conditioning and Refrigeration Institute (ARI) [2,3]. The entering dry bulb temperature for the outdoor coil for steady state and cyclic tests was $82^{\circ} \pm 0.3$ F DB and 20% relative humidity. The steady state tests were repeated for outdoor temperatures of 90° , 95° , and 100° F. The indoor conditions were set at $80^{\circ} \pm 0.3$ F DB and $60^{\circ} \pm 0.3$ F DP (67° F WB) for the wet coil test (A&B). For dry coil and cyclic tests, the dew point never exceeded at 32 F DP which was lower than the 37 F maximum specified in the test procedure [2,3]..

Indoor Test Section

The indoor test section is shown in Figure 2.2. Conditioned air flowed through a 22 inch by 34 inch cross section sheet metal duct which had one inch of insulation. A set of straighteners were used as the air entered this section. The air temperature was measured by a 16-element thermocouple grid before it entered into the coil. There were two dampers installed before and after the coil. The dampers were driven by two hydraulic actuators which were controlled by an "on-off" switch from the control room. After leaving the coil, the air flowed through another set of straighteners. Its temperature was then measured by a second 16-element thermocouple grid.

To accurately measure the dew point temperature, the dew point sensors had to be mounted in an air stream with velocities from 500 to 3000 fpm. An air sampler was constructed to sample the air entering the indoor coil. The sampler was a 4x6 inch duct with a fan at the end of the duct. The fan drew air through the duct where the dew point sensor

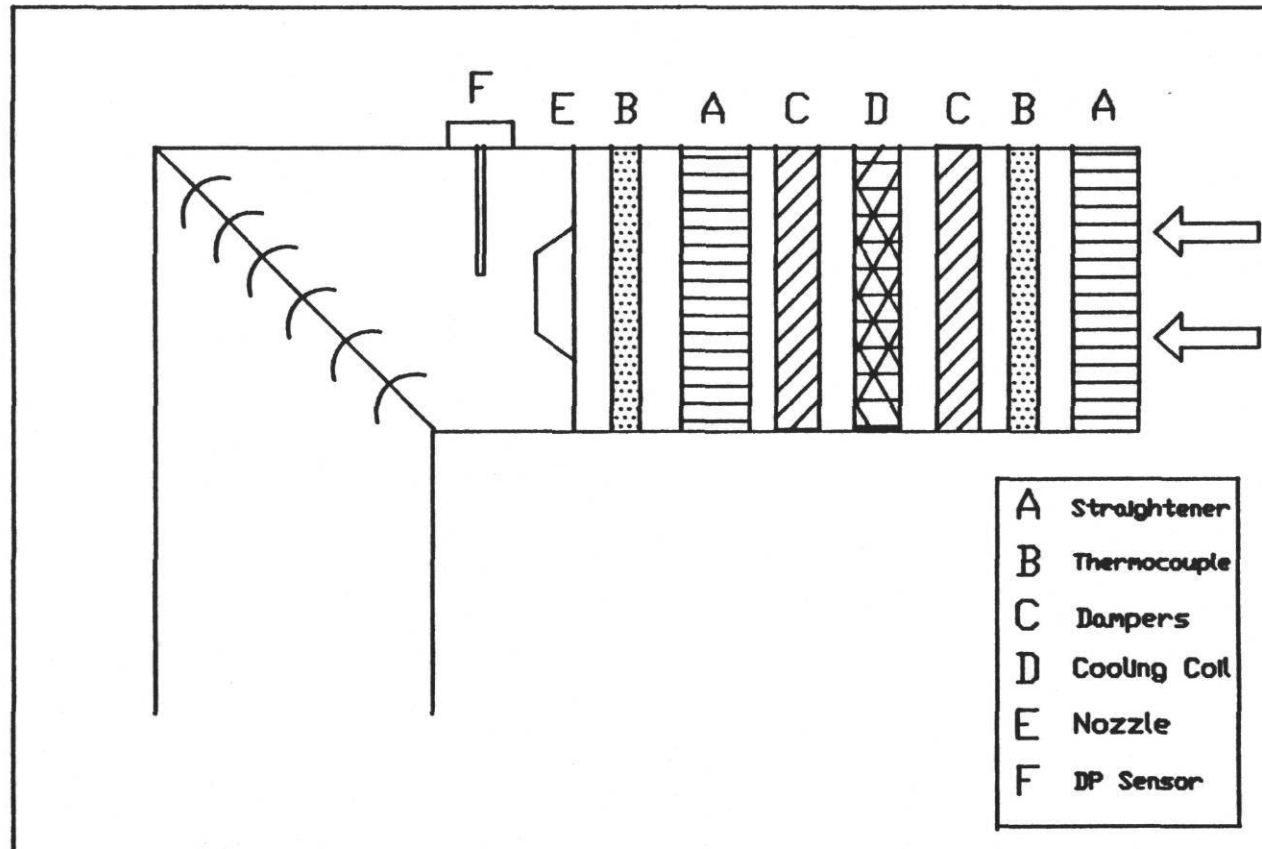


Figure 2.2 - Schematic of the indoor coil test section.

was mounted. The air flow through the duct was approximately 1700 fpm which was within the operating range of the sensor. A 12-inch nozzle was mounted after the second 16-element thermocouple grid to increase the velocity of air up to 1500 fpm for the down stream dew point sensor.

The air conditioner used in these tests was a 3-ton Trane air conditioner with orifice expansion. The outdoor and outdoor section model numbers were TTX736A100A1 and TWV742, respectively.

After leaving the test section, the air was drawn into an Air Movement and Control Association (AMCA) 210 flow chamber where the air flow was measured [4]. The chamber contains four American Society of Mechanical Engineers (ASME) air flow nozzles (one-8", two-5" and one-3") that could be used in any combination to accurately measure a flow range of 100 to 5000 cfm [4]. A booster fan mounted on the end of the chamber provided the air flow through the setup. The air flow was adjusted by operating a set of dampers mounted on the fan outlet. For the steady state and cyclic tests, two 5" nozzles were used in the chamber to achieve a pressure drop of 1.13" WG which was equivalent to 1150 cfm through the indoor test coil.

Outdoor Test Section

The outdoor test section included the compressor, the outdoor coil (condenser), and two refrigerant mass flow meters. A nominal 3-ton Trane air conditioner was used. The outdoor coil had one row of tubes with spine fins spaced at 20 per inch. The face area of the coil was 20.94 ft² with refrigerant tube sizes of 3/8". The outdoor fan was located on the top of the outdoor coil. The fan specifications are given in Table 2.1.

The temperature of the air leaving the outdoor coil was measured by a 6 element thermocouple grid. According to ARI standard 210/240-84 [3], the wet bulb temperature condition was not required when testing an air-cooled condenser which did not evaporate condensate.

Table 2.1 - Fan Specification

Fan Type	Propeller
Diameter (in)	22
Drive Type	Direct
CFM @ 0 in. w.g.	2735
Motor HP	1/4
Motor Speed RPM	825
F.L. Amps	1.9

Refrigerant Side

A schematic of the refrigerant circuit is shown in Figure 2.3. Refrigerant pressures were monitored at the 6 points shown with the use of 0-300 psig pressure transducers. To accurately measure the refrigerant temperatures and reduce the conduction effects of the copper tubing, eight thermocouple probes were installed in the refrigerant lines. The probes were 1/16" in diameter and mounted far enough into the flow of the refrigerant to minimize the tube conduction effects. Figure 2.5 shows a typical refrigerant temperature probe.

Refrigerant flow was measured with two Coriolis effect mass flow meters operating in parallel. As shown from Figure 2.4, the meters were placed on the liquid line after the condenser unit. The pressure drop across the flow meters was a maximum of 10 psi (for fully charged condition). This pressure drop was less than the 12 psi pressure drop acceptable by ASHRAE Standard 116-83 [5] (12 psi is the equivalent pressure drop for refrigerant at the test conditions experiencing the maximum allowed temperature drop of 3°F).

The valves shown in the refrigerant circuit diagram were lever-actuated shut-off valves. Several ball valves were mounted around all sections of the refrigerant circuit to allow easy disassembly of the unit without any loss of refrigerant charge. Charging taps in each section of the circuitry allowed purging and charging of each section independently.

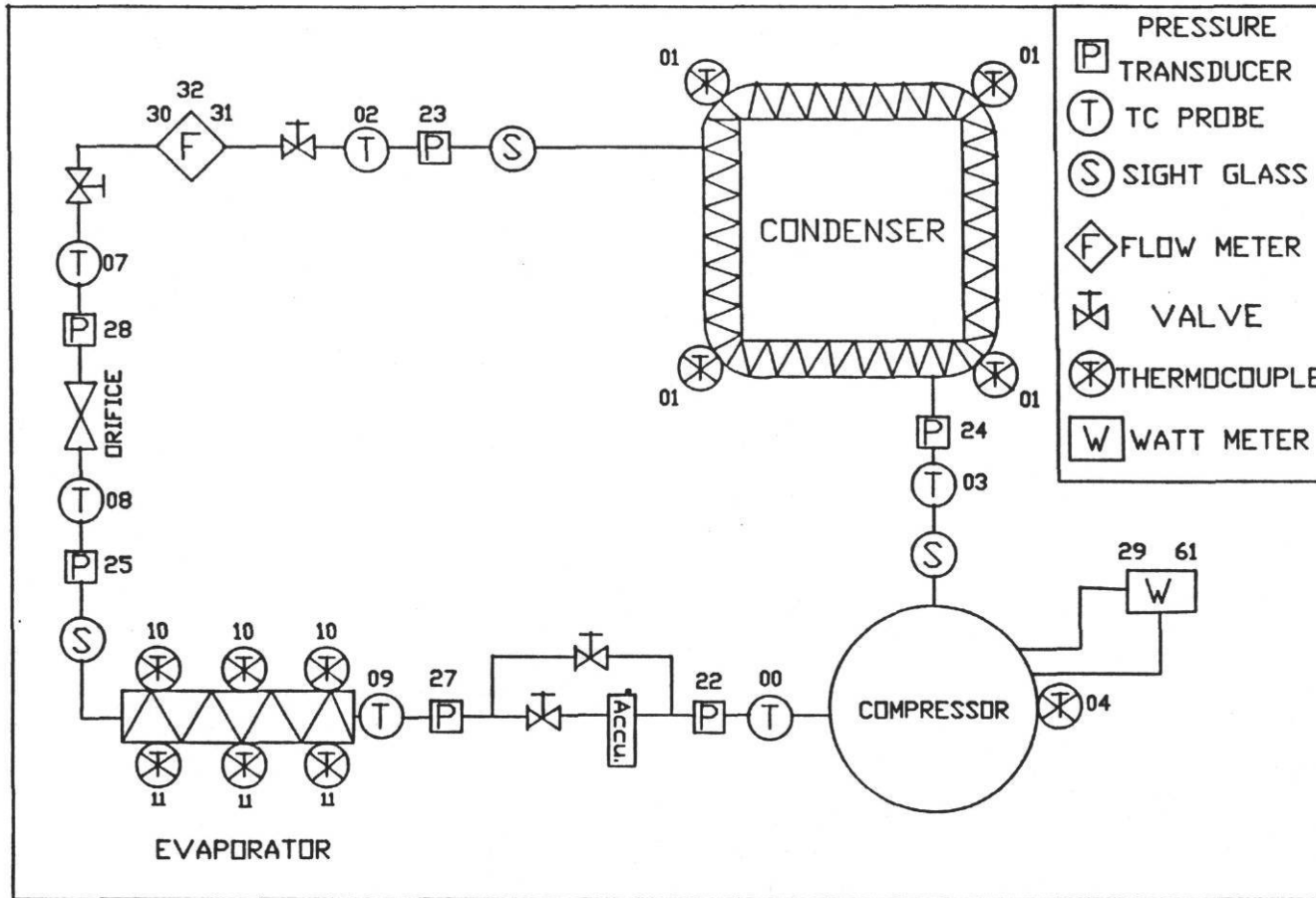


Figure 2.3 - Schematic of the refrigerant circuit with measurement locations.

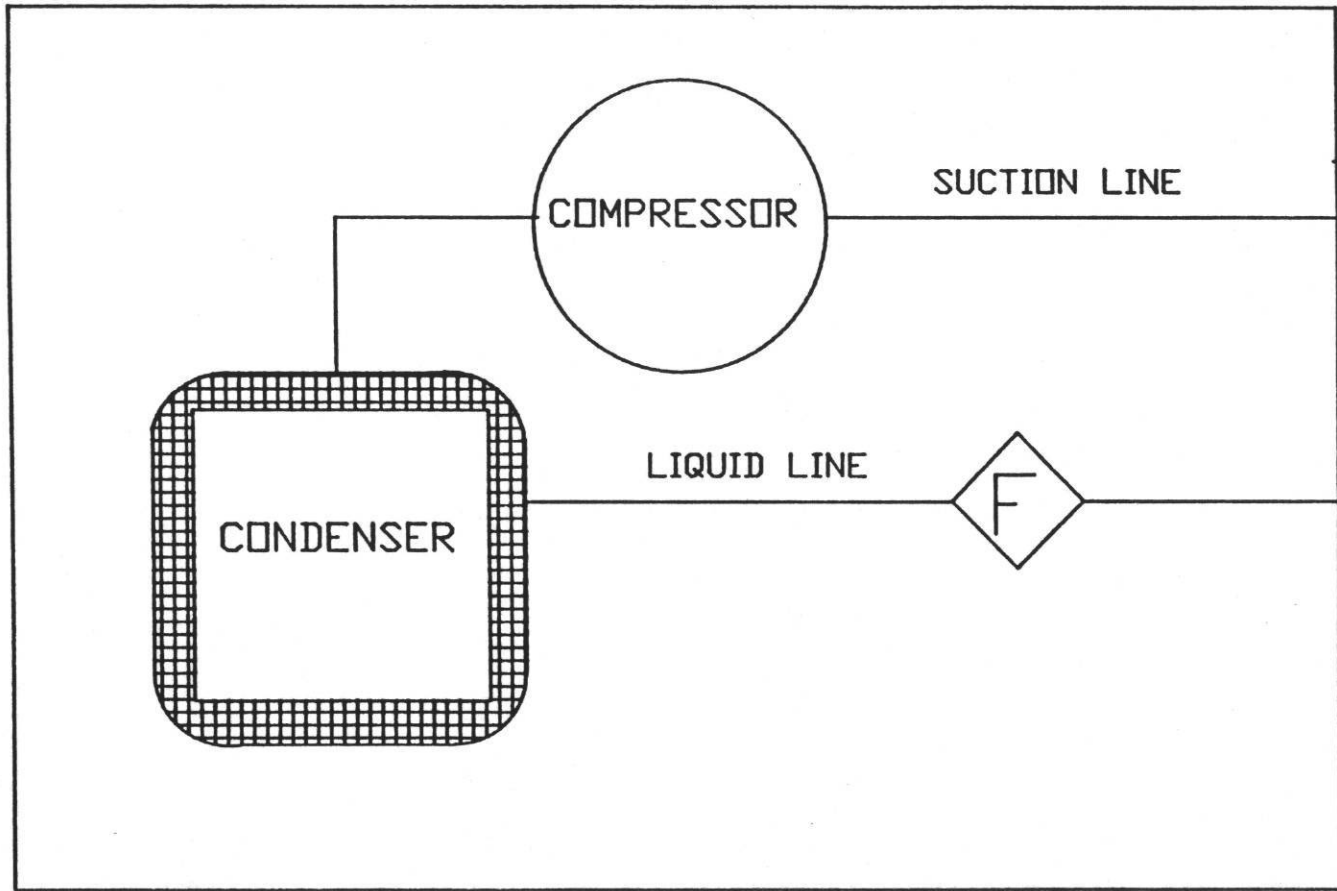


Figure 2.4 - Schematic showing the location of the refrigerant mass flow meters.

Data Acquisition

Sensor signals from the test points (Table 2.2) were collected and converted to engineering units by an Acurex (model Autocalc) data logger. The data logger handled millivolt and milliamp signals as well as larger voltages and frequency signals. During each test, the data processed by the data logger was transferred to a portable Compaq personal computer where it was stored on a 10 megabyte hard disk. The maximum collection and storage rate for the set of data channels used in a test was eight seconds per set. The scan rate was adjustable, so data from each test (cyclic and steady state) were collected every 15 seconds.

A feature of the data acquisition system was the continual display of data on the computer screen during testing. After completion of a test series, all data collected on the hard disk were backed up on floppy disks. FORTRAN programs were written and used to analyze the data on the PC. The programs included refrigerant and moist air property subroutines. These subroutines were used in calculation of air and refrigerant-side cooling capacities to provide an energy balance for data validation. Additional calculated properties and performance parameters for each test were plotted.

At the start of tests, the psychrometric rooms and the unit were started and allowed to run for a minimum of two hours to reach steady state conditions. Once steady state was reached for both the rooms and the system, the data for the steady state tests were recorded continuously for 20 minutes. The cooling cyclic tests were conducted by cycling the compressor 6 minutes "on" and 24 minutes "off". The capacity was measured for 8 minutes, six minutes of "on" time and two minutes longer until it reached zero. Electrical energy was measured for 6 minutes of "on" time. The dampers were shut off after first 8 minutes of the cyclic test to isolate the indoor coil.

Table 2.2 Description of Test Points Used
in the Test Set-Up

Channel	Sensor	Location
00	TC-Probe	Compressor Inlet
01	Thermocouple	Outdoor Room Temp.
02	TC-Probe	Condenser Outlet
03	TC-Probe	Compressor Outlet
04	Thermocouple	Compressor Shell Temp
05	Thermocouple	Before Nozzle-Chamber
06	Thermocouple	After Nozzle-Chamber
07	TC-Probe	Orifice Inlet Temp.
08	TC-Probe	Evap. Inlet Temp.
09	TC-Probe	Evap. Outlet Temp.
10	TC-Grid	DB Indoor Coil Outlet
11	TC-Grid	DB Indoor Coil Inlet
12	Thermocouple	Chilled Water Temp.
13-19		-- Not Used --
20	Dew-Point	Downstream Indoor Coil
21	Dew-Point	Upstream Indoor Coil
22	Pressure Trans.	Compressor Inlet
23	Pressure Trans.	Condenser Outlet
24	Pressure Trans.	Compressor Outlet
25	Pressure Trans.	Evaporator Inlet
27	Pressure Trans.	Evaporator Outlet
28	Pressure Trans.	Orifice Inlet
29	Watt Trans.	208 VAC (single phase)
30	Flow Meter	Refr. Liquid Line
31	Flow Meter	Refr. Liquid Line
32		Sum of 30 & 31
33-60		-- Not Used --
61	WattHr Trans.	Compressor Power

Proper and Improper Refrigerant Charging Procedures

The superheat near the outdoor quick attach was used to determine the nominal full charge of refrigerant in the system. The recommended superheat was 10 F for full charge at an outdoor temperature of 95 F DB and indoor temperatures of 80 F DB and 67 F WB. Three orifice sizes were used: 0.067, 0.071, and 0.075 inches, respectively. The full charge for each is shown in Table 2.1 along with the actual superheat attained for the full charge. The superheat values varied slightly from the nominal 10 F for two reasons. First, charge

Table 2.3 - Refrigerant charge and actual superheat attained for each orifice size.

Orifice Size (in)	Refrigerant Charge (oz)	Superheat (F)
0.067	150	11.4
0.071	136	8.5
0.075	125	12.1

was added in one ounce increments. In some cases, the superheat was observed to change by as much as 3 to 4 F with the addition or removal of 1 ounce of refrigerant. Second, small fluctuations (± 0.2 F in dew point) in the humidity of the air moving over the indoor coil created as much as ± 2 F swings in the superheat.

Once the full charge was determined (140 ounces), a set of tests was performed at that charge. The system was then evacuated of refrigerant. Refrigerant was then added in increments (20% undercharging, 10% undercharging, etc.) to cover the full range of under/overcharging conditions for the particular orifices being tested.

The 0.071 inch orifice was designated the "nominal" size orifice. It underwent the most tests for different charging conditions. Table 2.4 shows the steady-state tests used with the nominal orifice.

Table 2.4 - Steady-State Tests performed for the 0.071 inch orifice

Charge	OUTDOOR TEMPERATURE (F)			
	82	90	95	100
+20%	X		X	
+10%	X	X	X	X
+ 5%	X		X	X
PROPER	X	X	X	X
- 5%	X		X	X
-10%	X	X	X	X
-20%	X		X	

The tests conducted for the "nominal" size orifice included the steady state tests shown in Table 1 as well as the standard DOE/ARI tests (A-D) to determine SEER[2]. The DOE/ARI tests were conducted for each charge shown in Table 2.4 and involved a total of seven sets of tests.

The other two orifices (0.067 and 0.071 inches) each underwent a limited set of steady-state tests (Table 2.5). One set of the DOE/ARI tests for the proper charge were performed for the two orifices.

Table 2.5 - Steady-State Tests performed for the 0.067 and 0.071 inch orifice

Charge	OUTDOOR TEMPERATURE (F)			
	82	90	95	100
+10%	X		X	
+ 5%	X		X	
PROPER	X	X	X	X
- 5%	X		X	
-10%	X		X	

References

1. M. Farzad and D. O'Neal, "An Evaluation of Improper Refrigerant Charge on the Performance of a Split System Air Conditioner with Capillary Tube Expansion", ESL/CON/88-1, Energy Systems Laboratory, Texas A & M University, July 1988.
2. Department of Energy, "Test Procedures for Central Air-Conditioners, Including Heat Pumps", Federal Register, pp. 76700-76723, Vol. 44, No. 249, 1979.
3. "Standard for Unitary Air-Conditioning and Air-Source Heat Pump Equipment", Standard 210/240, Air Conditioning and Refrigeration Institute, 1985.
4. "Laboratory Methods of Testing Fans for Rating", ANSI/ASHRAE Standard 51-1985 (ANSI/AMCA 210-85).
5. "Methods of Testing for Seasonal Efficiency of Unitary Air-Conditioners and Heat Pumps", ANSI/ASHRAE Standard 116-1983.

CHAPTER 3

NOMINAL SIZE ORIFICE RESULTS

The refrigerant charge in a system was systematically varied to determine its effect on the capacity, EER, SEER, and coefficient of degradation (C_D) of the Trane central air conditioner provided to the Energy Systems Laboratory. The results for the nominal orifice (0.071 inch) are presented below. The results include overall system performance data and detailed system data (subcooling, mass flow, etc.). (power, capacity, etc.).

System Performance Data

Four variables were used to quantify the overall performance of the unit: total electrical power consumption, total capacity, Energy Efficiency Ratio (EER), and Seasonal Energy Efficiency Ratio (SEER).

The total electricity power consumption by the system is the combination of power consumed by the indoor and outdoor sections. The outdoor section power was measured directly with a watt-hour meter. The indoor fan power was calculated based on 365 watt per 1000 cfm of air because the test unit operated without an indoor unit fan [1,2,3]. The power increased with both outdoor temperature and increasing charge (Figure 3.1).

The total capacity of the unit was measured on both the air and refrigerant side of the evaporator. However, only data from the air-side are presented in this report. The indoor coil capacity was calculated using the air-enthalpy method found in ASHRAE Standard 116-1983 [1]. In the air-enthalpy method, the steady state capacity of the indoor coil was determined from:

$$\text{Capacity} = \frac{\text{cfm}}{v} \times (h_2 - h_1)$$

where,

- h_1 = Enthalpy of air entering the indoor coil (Btu/hr),
- h_2 = Enthalpy of the air leaving the indoor coil (Btu/hr),
- cfm = cubic feet per minute of dry air passing through the indoor coil, and
- v = specific volume of the air passing through the coil (ft^3/lb).

Power Consumption as a Function
of Temperature and Charge
orifice (0.071)

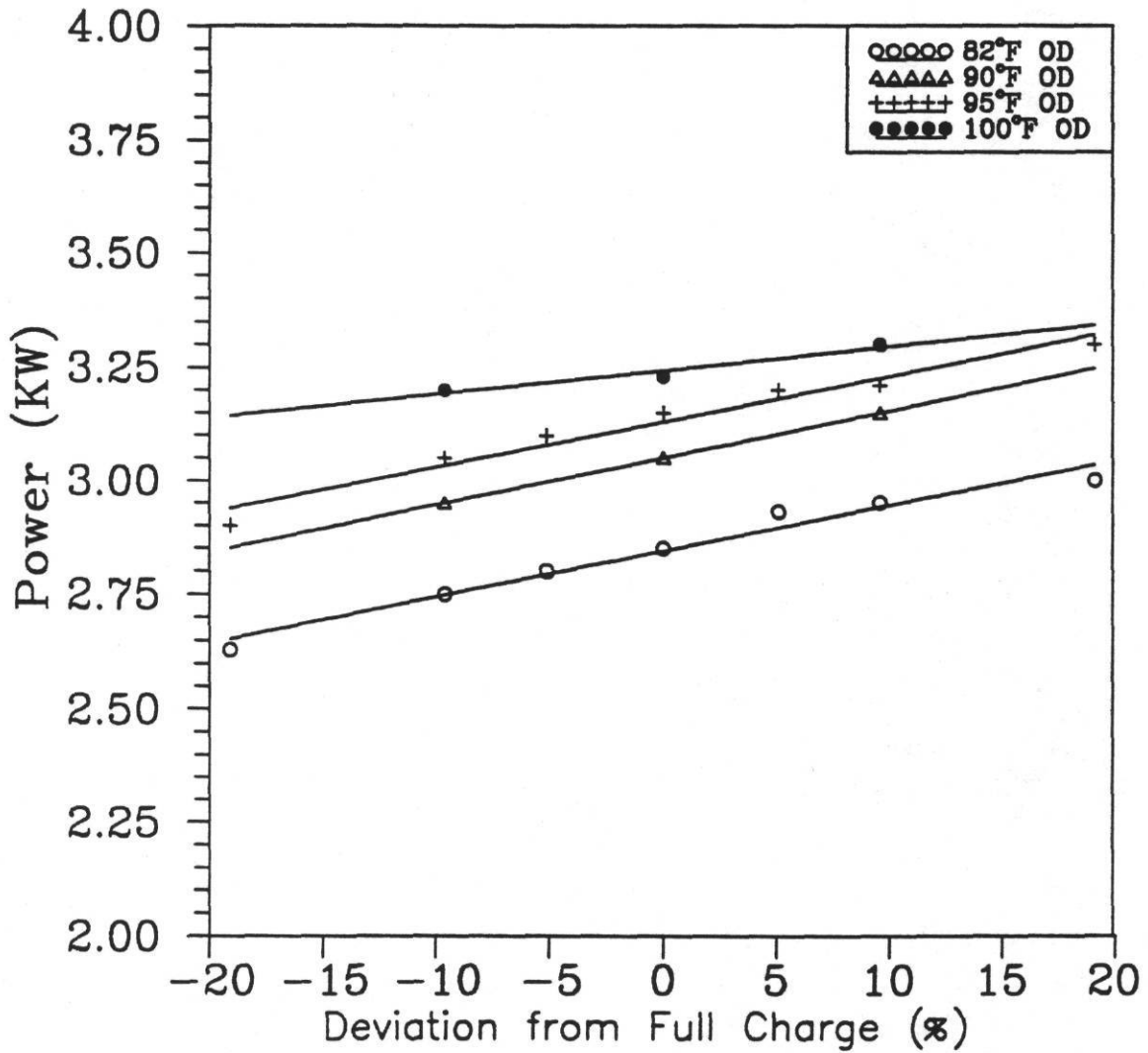


Figure 3.1 - Power consumption for the nominal sized orifice.

Values h_1 , h_2 , and v were obtained from methods contained in the ASHRAE 1985 Fundamentals Handbook [4]. The airflow calculations were done using a method provided in ANSI/ASHRAE Standard 51-1985[5].

The refrigerant side capacity was calculated by multiplying the refrigerant mass flow rate by the change in enthalpy of the refrigerant entering and leaving the indoor coil. The enthalpy of the refrigerant was calculated using subroutines developed by Kartsounes and Erth[6].

To verify the calculations for the air-side capacity, an energy balance was performed on the indoor coil. For all tests, the energy balance on the air side was within +4% of that on the refrigerant side. These results conformed to the requirements in the ARI 210 test procedure[2].

The capacity data (Figure 3.2) had more scatter than the power data in Figure 3.1. The capacity dropped as the charge decreased from full charge. The capacity showed a peak that was dependent on the outdoor temperature. The capacity appeared to peak between 10 and 20% overcharge for 82 F, between 5% and 10% overcharge for 95 F, and at approximately 5% overcharge for 100 F.

The EER showed a strong dependence on outdoor temperature, but varied little with charge (Figure 3.3). For instance, at 95 F, the EER varied from 9.1 at 20% undercharge to 8.6 at 20% overcharge. This behavior contrasts quite dramatically with the behavior of the capillary tube expansion system tested earlier[5]. In those tests, the EER at 95 F, dropped from a peak of 9.4 at 5% undercharging to lows of 7.8 for 20% undercharging to 7.9 for 20% overcharging.

The DOE test procedure requires three steady state tests (A,B,C) and one cyclic test (D). Tests A & B are steady state wet coil tests at 95° and 82° F DB outdoor room temperatures, respectively. Test (D) is a steady state dry coil test at 82° F DB outdoor room temperature. The calculation of the unit's SEER with a single-speed compressor and single-speed condenser fan is done in accordance with the ARI/DOE test procedure [2,3]. First, a cyclic-cooling-load factor (CLF) is determined from:

$$CLF = Q_D / (Q_C t_C)$$

Q_D is the total cooling capacity of test D and Q_C is the steady state cooling capacity of test C. t_C is duration of time (hours) for one complete cycle consisting of one compressor "on" time and one compressor "off" time. The degradation coefficient, C_D , is the measure of the

Total Capacity as a Function of
Temperature and Charge
orifice (0.071)

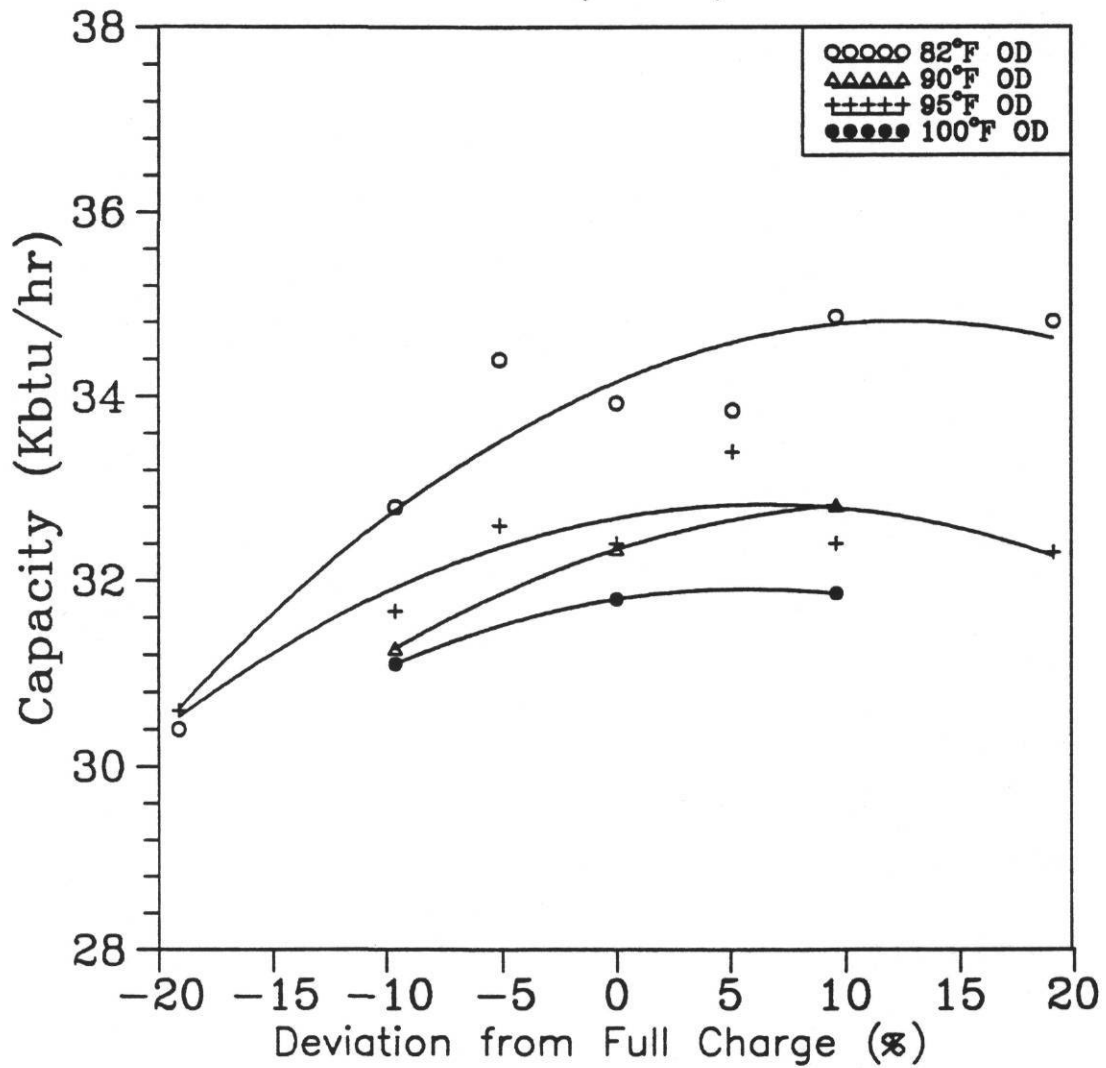


Figure 3.2 - Cooling capacity for the nominal sized orifice.

Energy Efficiency Ratio as a Function of Temperature and Charge orifice (0.071)

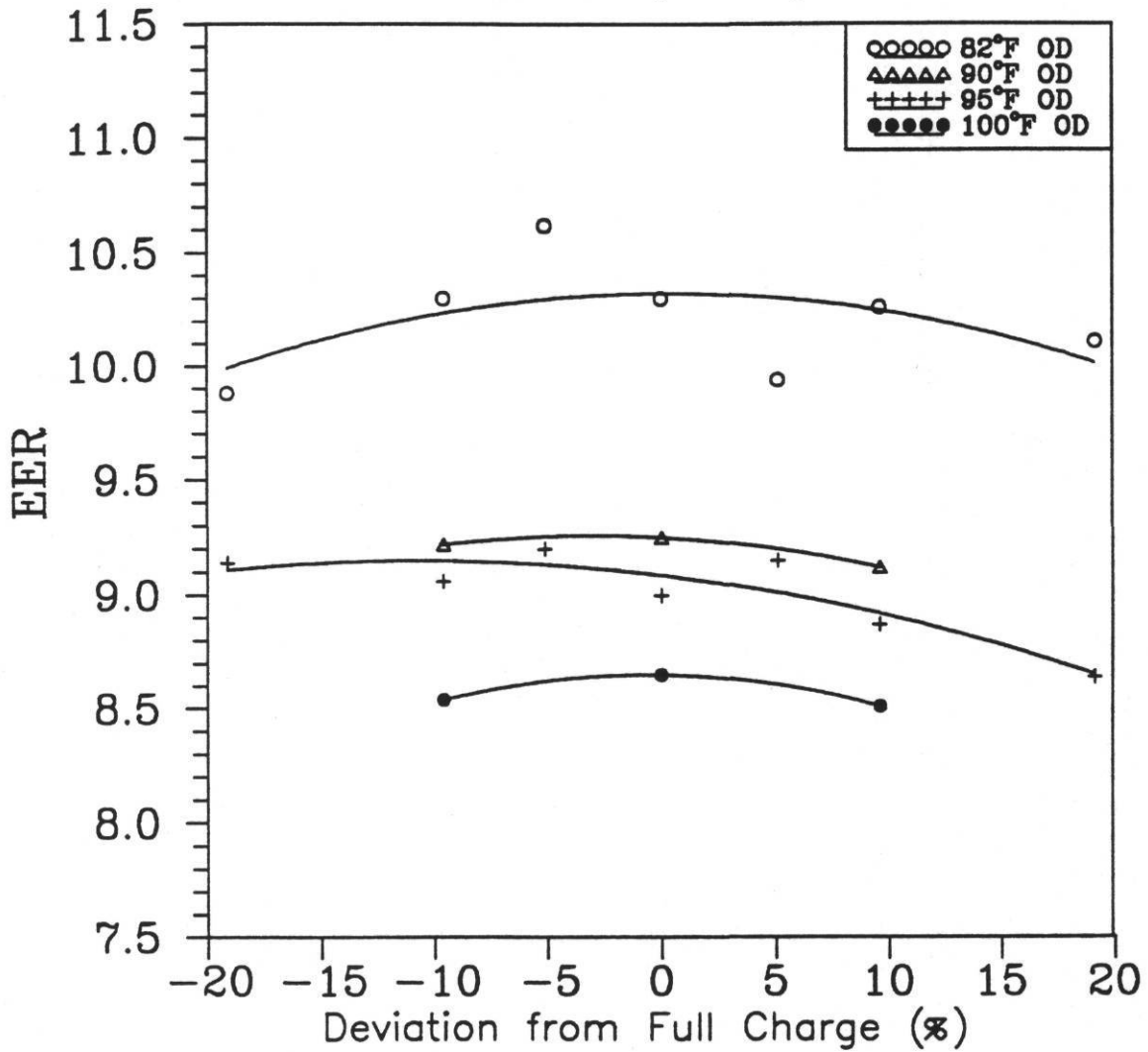


Figure 3.3 - Steady-state energy efficiency ratio with the nominal sized orifice.

efficiency loss due to the cyclic of the unit. C_D is calculated from:

$$C_D = (1 - EER_D/EER_C) / (1 - CLF)$$

EER_D and EER_C are the energy efficiency ratios of tests D and C, respectively.

The SEER is then determined from a bin hours cooling method calculated based on representative use cycle of 1000 cooling hours per year. A 95°F cooling outdoor design temperature was used. In accordance with ARI test procedure, the cooling building load size factor 1.1 (10% oversizing) was used.

The SEER peaked at 9.9 for 5% undercharging and and decreased to approximately 9.3 (6% drop) for both 20% over and undercharging (Figure 3.4). As with the capacity, the degradation in SEER with respect to under/overcharging was much smaller with the orifice than the capillary tubes. The SEER for capillary tubes dropped by 20% from its peak value for a 20% undercharge and by 10% for a 20% overcharge.

The coefficient of degradation (C_d) increased from 0.116 at 20% undercharging to 0.13 at 10% undercharging and then dropped to 0.09 for 20% overcharging (Figure 3.5). The trend of a low C_d at low charge, reaching a plateau, and then decreasing with increasing charge is similar to the trends found in the earlier study with the capillary tube system. However, the absolute values of C_d were larger for the capillary tube unit which varied from 0.15 to a maximum of 0.25.

The sensible heat ratio (SHR) is defined as the ratio of the sensible capacity to the total capacity of the unit. The SHR for the base system showed no clear or definitive trends (Figure 3.6). At both 82 F and 95 F outdoor temperatures, the SHR showed a slight increase with increasing charge. For the other two temperatures (90 F and 100 F), there was a small decrease. However, the 90 F and 100 F temperatures only included 3 charge conditions (-10%, full, and +10%). Because of the small number of data points and the observed scatter, an addition (or reduction) of one data point could change the direction of the trends observed. The SHR for the orifice system showed less variation with temperature and charge than did the capillary tube system tested earlier. For instance, the SHR varied from a low of 0.727 (20% undercharge, 82 F) to a high of 0.820 (100 F, 20% overcharge) for the capillary tube system. The SHR for the orifice system only varied from 0.728 (5% undercharge, 82 F) to 0.785 (10% undercharge, 90 F).

Seasonal Energy Efficiency Ratio as a Function of Charge

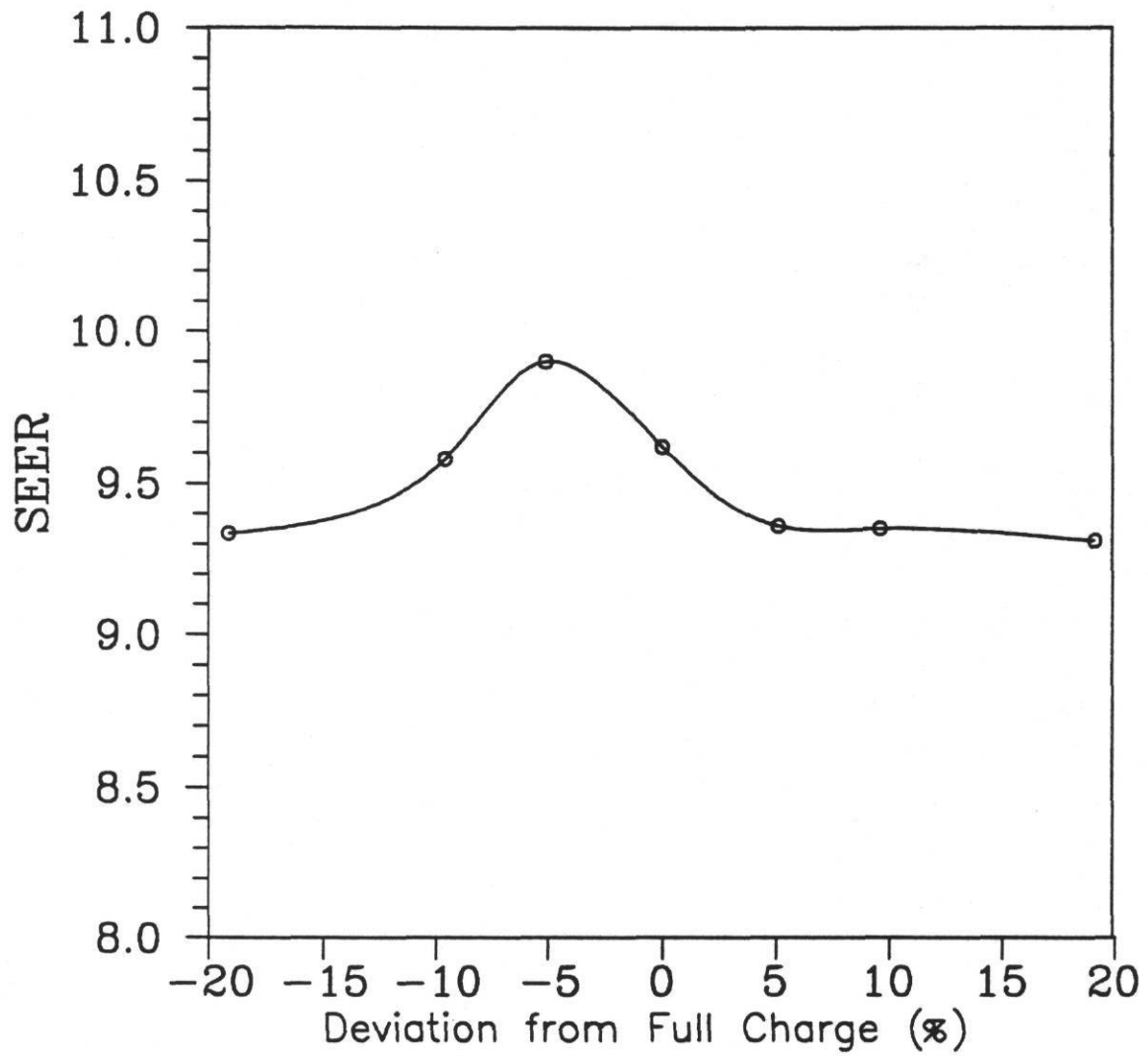


Figure 3.4 - Seasonal energy efficiency ratio with the nominal sized orifice.

Coefficient of Degradation as a Function of Charge

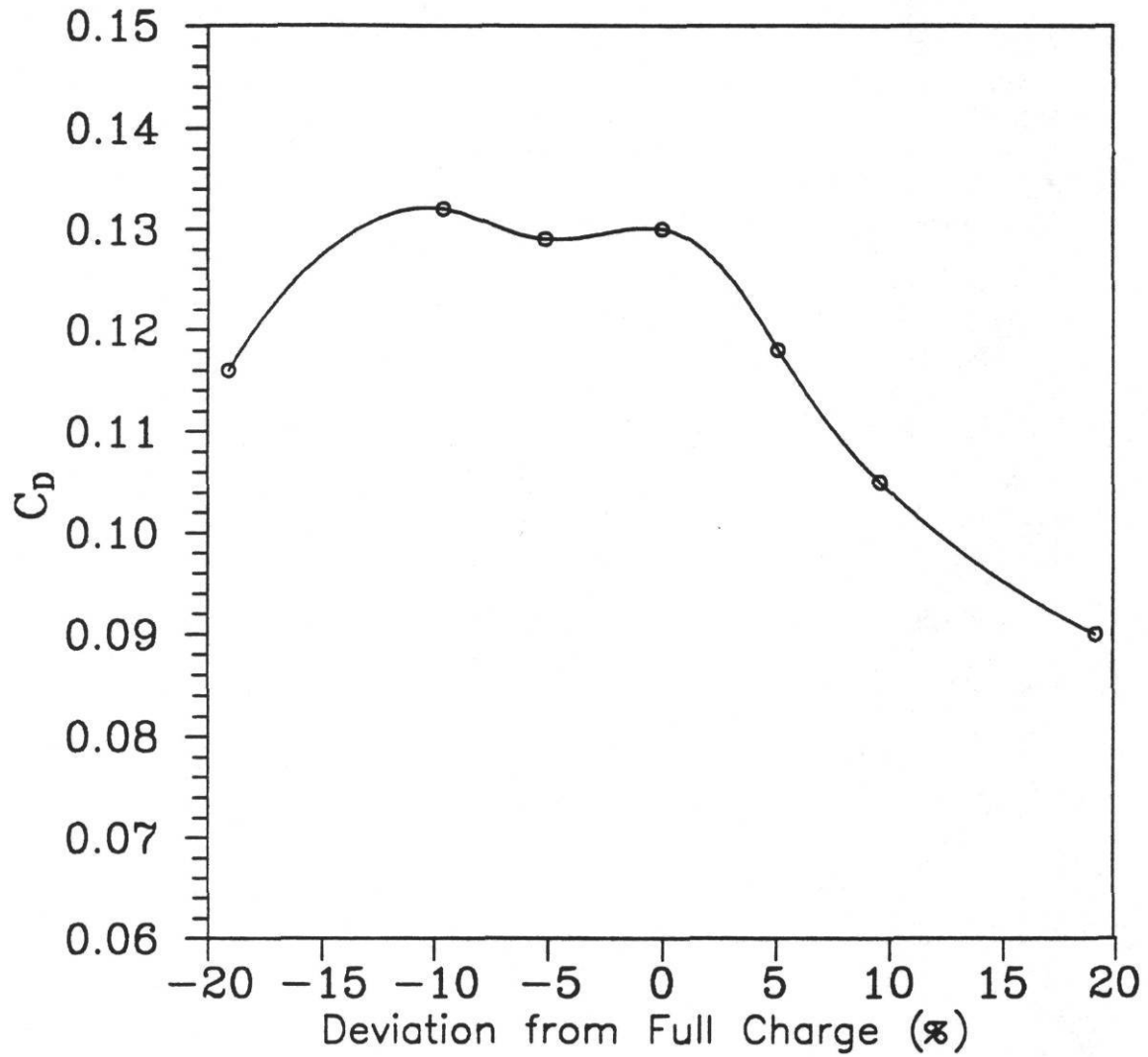


Figure 3.5 - Coefficient of Degradation with the nominal sized orifice.

Sensible Heat Ratio as a Function
of Charge and Outdoor Temperature
orifice (0.071)

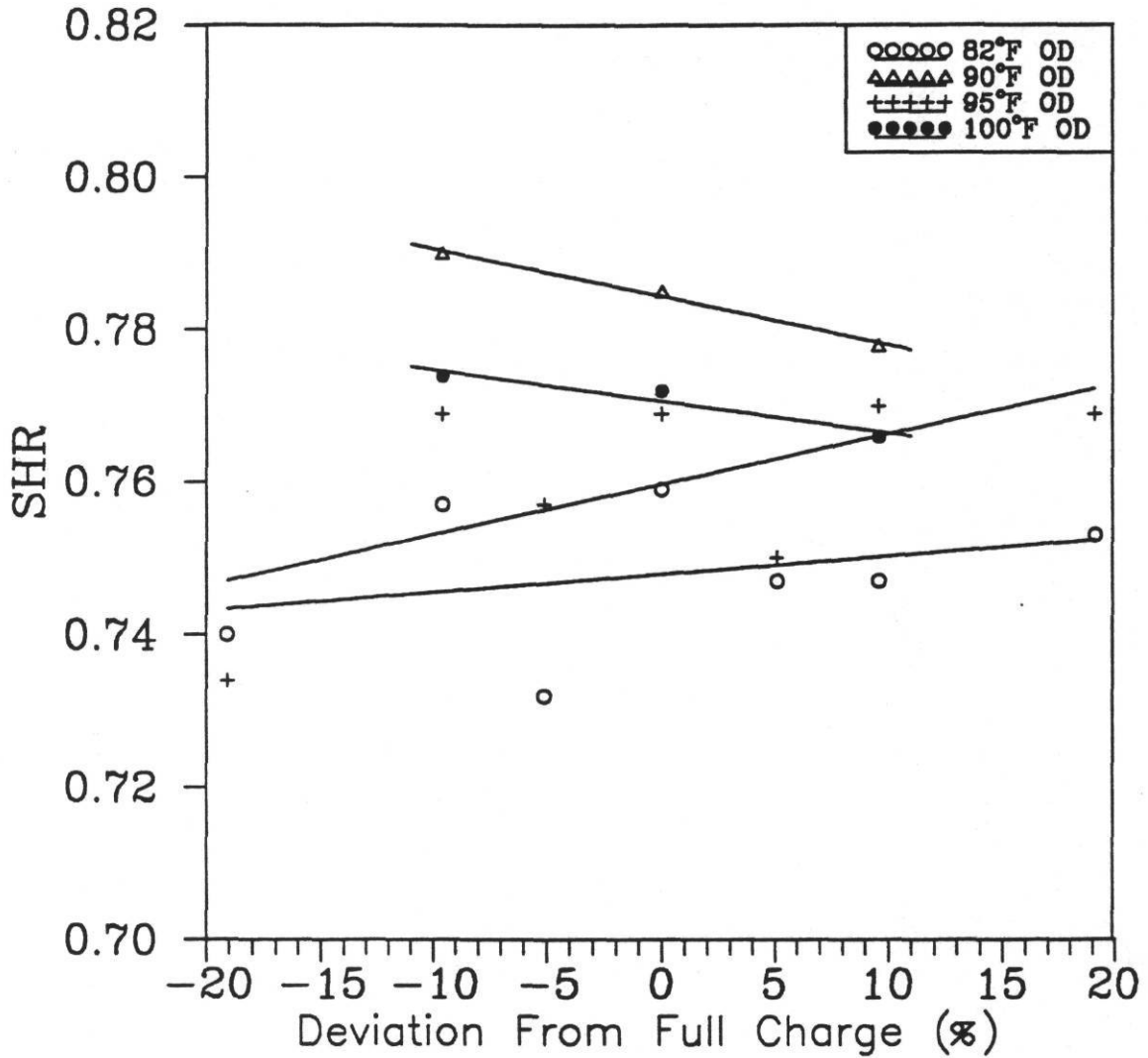


Figure 3.6 - Sensible heat ratio with the nominal sized orifice.

Detailed System Data

The superheat near the compressor disconnect was extremely sensitive to charge (Figure 3.7). At full charge the superheat was at 8 F for 95 F outdoor dry bulb temperature. A drop in charge of 5% (7 ounces) increased the superheat to 19 F. The superheat dropped 3 F at 10% overcharge and remained at 3 F for 20% overcharge. For overcharges of 10% and greater, the refrigerant was superheated at the outlet of the evaporator. Thus, the 3 F superheat reflects the pressure drop between the evaporator outlet and the location where superheat was measured near the compressor inlet.

With a fixed expansion device such as an orifice, the refrigerant flow rate should increase with an increase in pressure at the inlet to the orifice or with larger subcooling. Refrigerant flow rate increased rapidly with increasing inlet pressure (Figure 3.8). The pressure at a given temperature was dependent on the refrigerant charge. The data shown in Figure 3.8 for a given temperature correspond to specific under/overcharging conditions. For instance, there are two lines with 7 data points (82 F and 95 F outdoor conditions). The smallest flow rate at 95 F (7.1 lb/hr) corresponds to a 20% undercharge, the next largest flow rate (7.9 lb/hr) to 10% undercharge, etc. The other two line with 3 data points only have 10% undercharge, proper charge, and 10% overcharge points with the smallest flow rate corresponding to the 10% undercharging.

Another variable affecting flow rate is the subcooling. Subcooling increased with increasing charge for all outdoor temperatures (Figure 3.9). For 95 F outdoor temperature, the subcooling increased from 1 F at 20% undercharge to 12.5 F for 20% overcharge. For the same range in charge, the pressure at the orifice inlet increased from 228 psia to 245 psia. Thus, with both pressure and subcooling increasing, the flow rate increases.

Superheat Temperature as a Function
of Temperature and Charge
orifice (0.071)

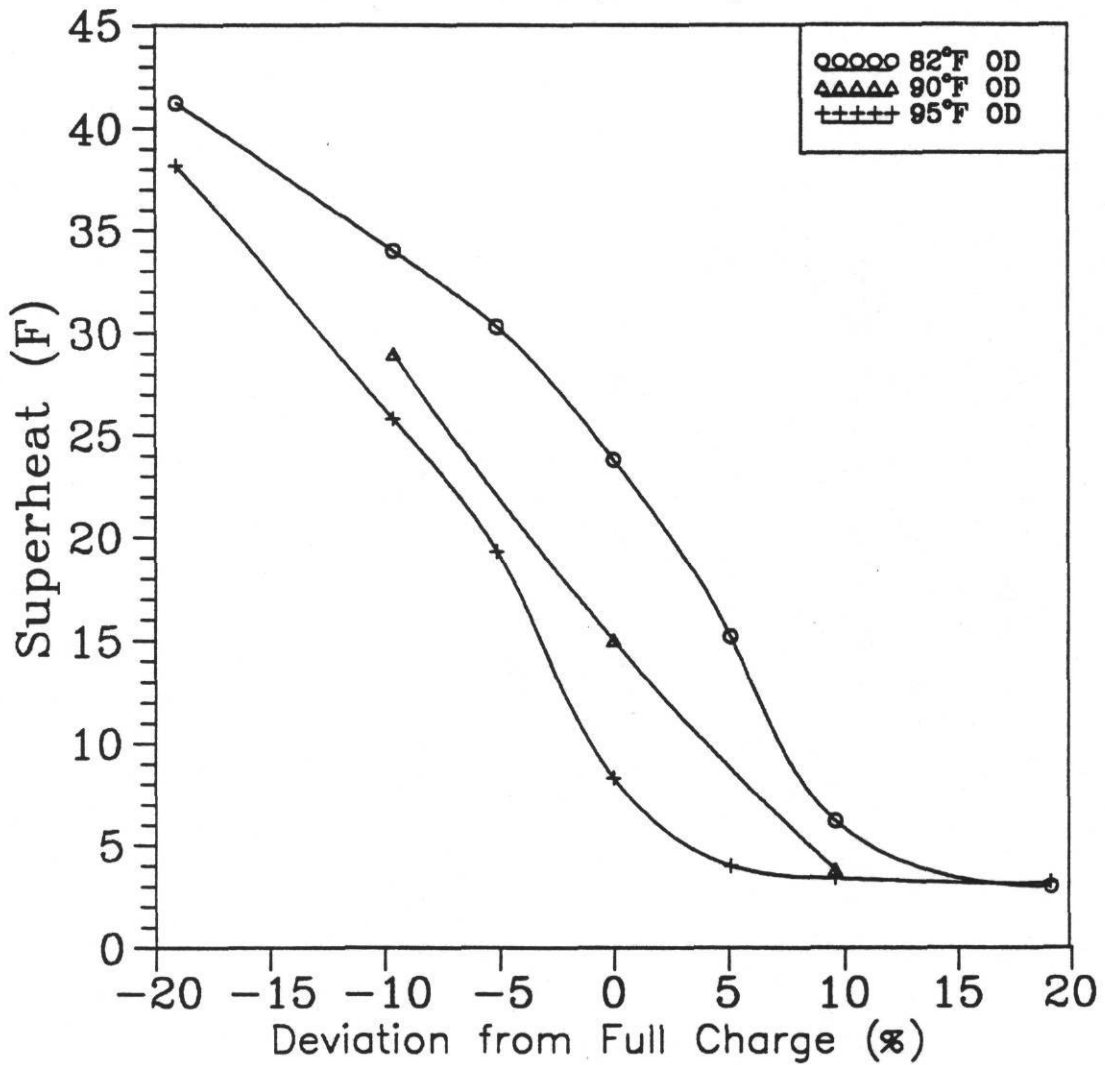


Figure 3.7 - Superheat near the quick disconnect
with the nominal sized orifice.

Refrigerant Flow Rate as a Function of Orifice Inlet Pressure orifice (0.071)

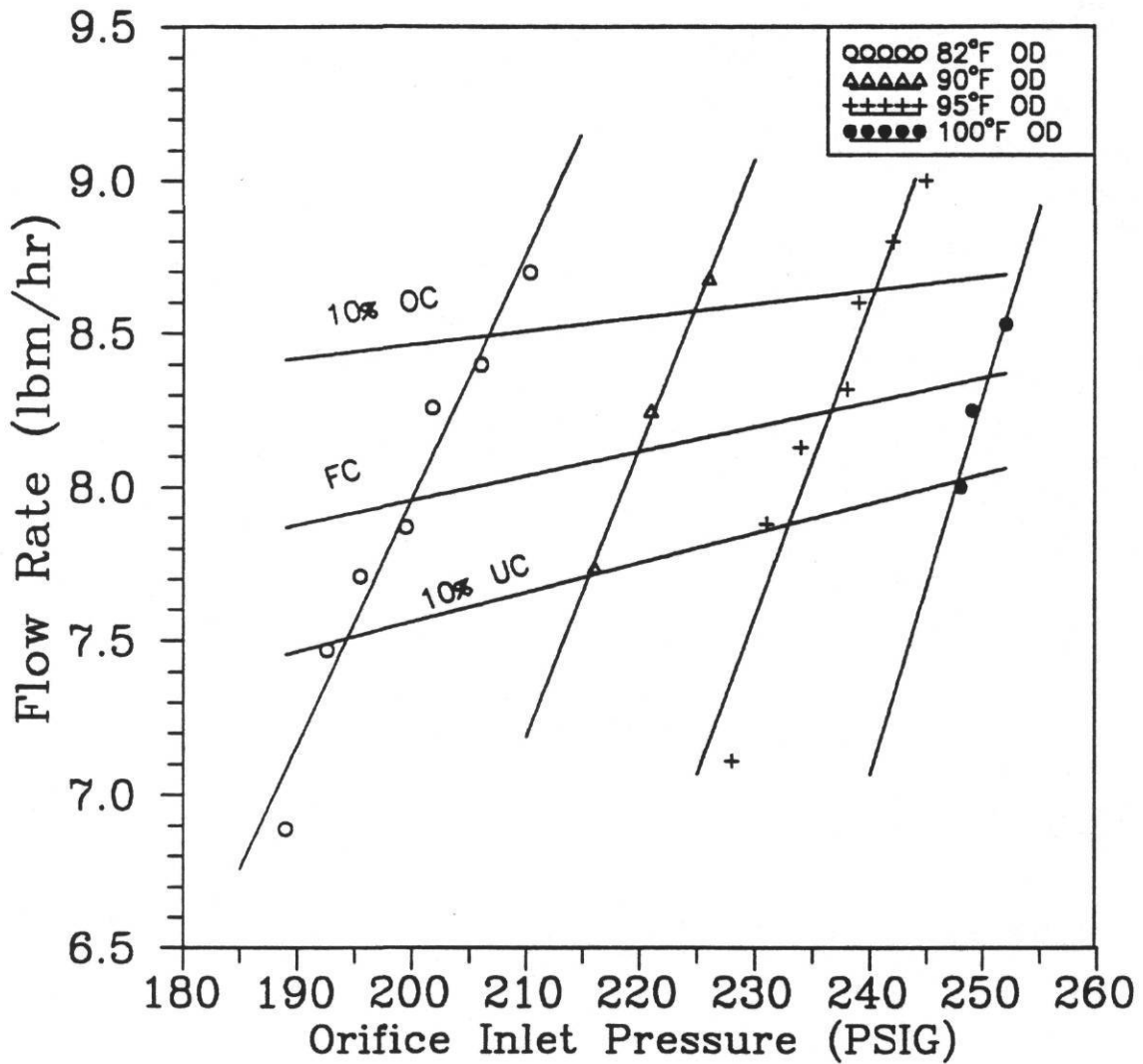


Figure 3.8 - Refrigerant flow with the nominal sized orifice.

Subcooled Temperature as a Function of Temperature and Charge orifice (0.071)

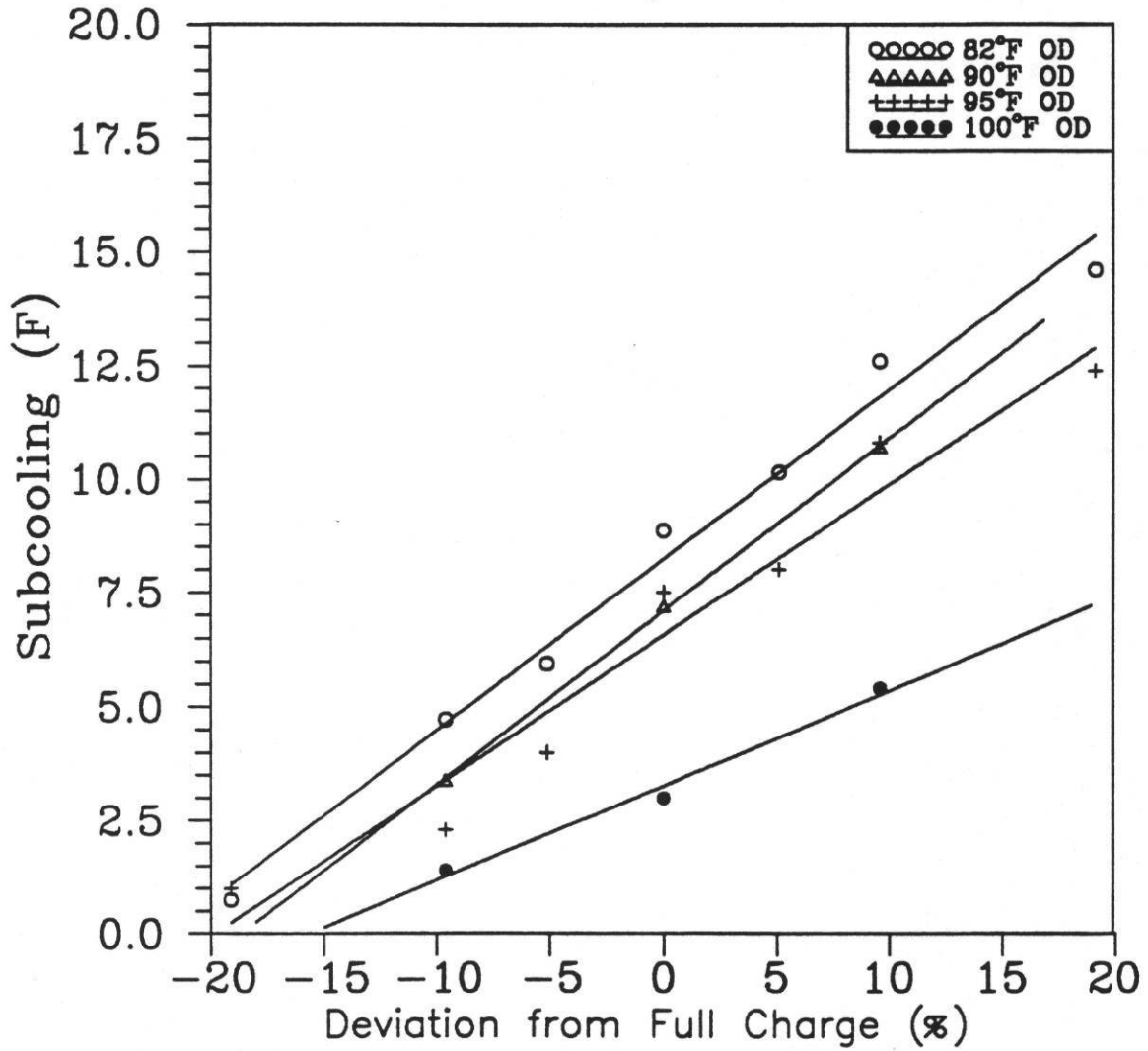


Figure 3.9 - Subcooling at the orifice inlet with the nominal sized orifice.

References

1. Methods of Testing for Seasonal Efficiency of Unitary Air-Conditioners and Heat Pumps", ANSI/ASHRAE Standard 116-1983.
2. "Standard for Unitary Air-Conditioning and Air-Source Heat Pump Equipment", Standard 210/240, Air Conditioning and Refrigeration Institute, 1985.
3. Department of Energy, "Test Procedures for Central Air-Conditioners, Including Heat Pumps", Federal Register, pp. 76700-76723, Vol. 44, No. 249, 1979.
4. American Society of Heating, Refrigerating and Air-Conditioning Engineers, ASHRAE Handbook: 1985 Fundamental, p. 6.12-13, Atlanta, Georgia, 1985.
5. "Laboratory Methods of Testing Fans for Rating", ANSI/ASHRAE Standard 51-1985 (ANSI/AMCA 210-85)
6. Kartsounes, G.T., and Erth, R.A., "Computer Calculations of the Thermodynamic Properties of Refrigerants 12, 22, and 502", ASHRAE Transactions, pp. 88-103, 1971.
7. Farzad, M. and D.L. O'Neal, "An Evaluation of Improper Refrigerant Charge on the Performance of a Split System Air Conditioner with Capillary Tube Expansion", ESL/CON/88-1, Energy Systems Laboratory, Texas A & M University, July 1988.

CHAPTER 4

RESULTS FOR ALTERNATE ORIFICES

Two other orifices (0.067 and 0.075 inches in diameter) underwent limited tests to assess system sensitivity to refrigerant charge. Tests for charge sensitivity were limited to $\pm 10\%$ of full charge for the two orifices (See Chapter 2 for tests run on these orifices). Many of the trends in performance were similar to those of the nominal size (0.071 inch) orifice. Power consumption appeared to linearly increase with charge for all temperatures (Figures 4.1 and 4.2) in a manner similar to the nominally sized orifice. Power for the 0.075 inch orifice was approximately 0.1 kw less than the 0.067 inch orifice for all temperatures and charges.

Capacities showed an increase with increasing charge over the limited range for these tests (Figure 4.3 and Figure 4.4). The 0.067 inch orifice did not appear to reach a maximum capacity with charge like the 0.071 and 0.075 inch orifice did. The larger orifice dropped more in capacity at 10% undercharging than did the 0.067 inch orifice. At 95 F, the 0.075 inch orifice dropped 9% in capacity at 10% undercharging compared to the capacity at proper charge (32.0 kBtu/hr). In contrast, the 0.067 inch orifice dropped 2% from 31.9 kBtu/hr for the proper charge.

The steady state EERs with both sized orifices showed little variation with charge from 10% under to 10% overcharged (Figures 4.5 and 4.6). For charges larger than 5% undercharging, the 0.075 inch orifice produced EERs that were generally 0.1 to 0.2 Btu/wh greater than the 0.067 inch orifice.

The superheat near the compressor inlet showed similar changes with decreased charge for both the 0.067 and 0.075 inch orifices (Figure 4.7 and 4.8). For instance, the superheat went from 11 F at full charge to 29 F for 10% undercharge for the 0.067 inch orifice. For the 0.075 inch orifice, the superheat went from 12 F to 34 F.

The 0.075 inch orifice system produced a much smaller amount of subcooling at the outlet of the condenser than did the 0.067 inch system (Figures 4.9 and 4.10). One possible explanation for the smaller subcooling for the smaller subcooling for the larger orifices was the differences in condensing pressures for the two orifices. The inlet pressure to the 0.075 inch orifice was typically 10 to 20 psi less than that for the 0.067 inch orifice for a given outdoor air temperature. For instance, at 95 F and full charge, the inlet pressure to the orifice was 249 psia with

Power Consumption as a Function
of Temperature and Charge
orifice (0.067)

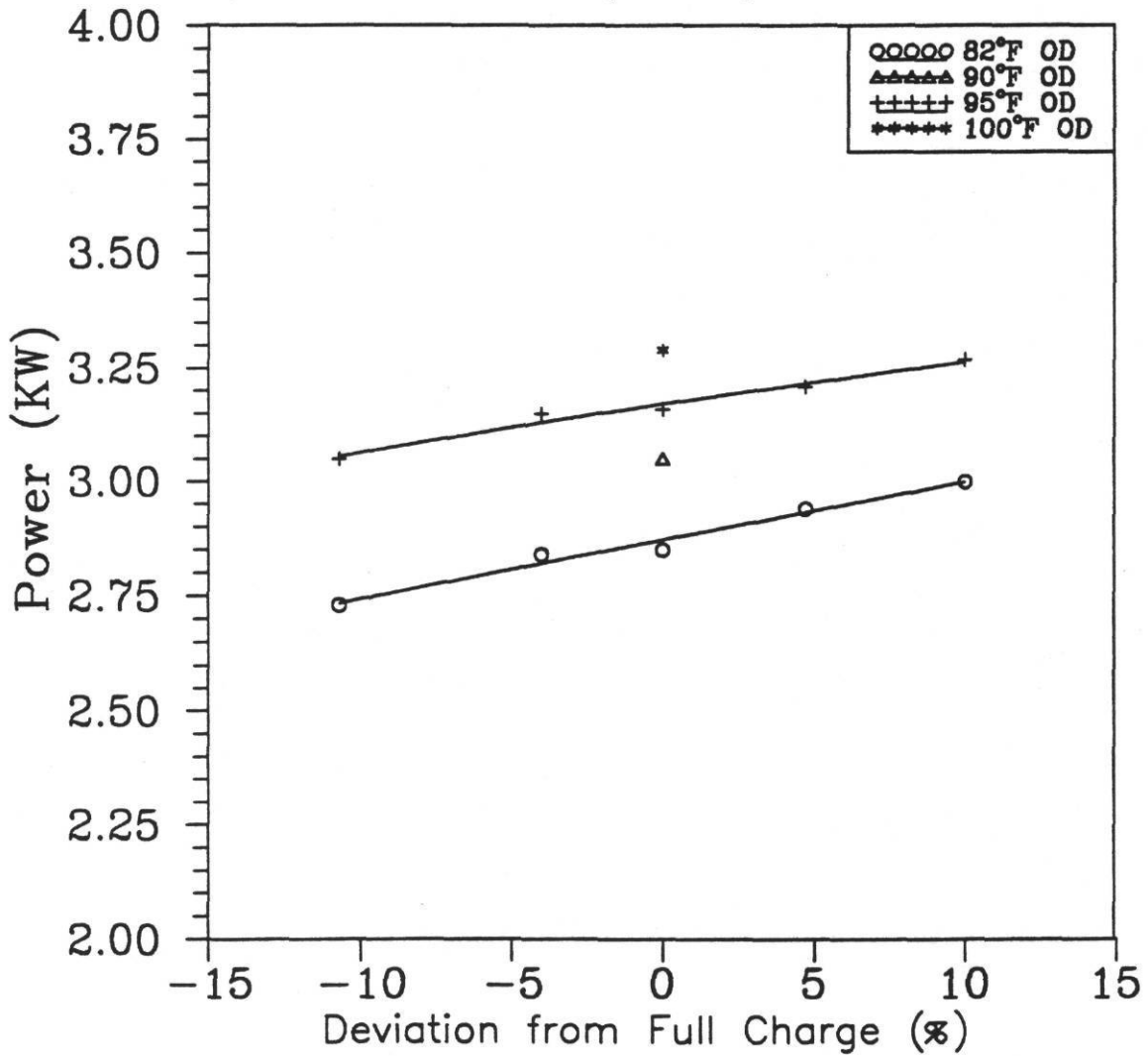


Figure 4.1 - Power consumption with the 0.067 inch diameter orifice.

Power Consumption as a Function
of Temperature and Charge
orifice (0.075)

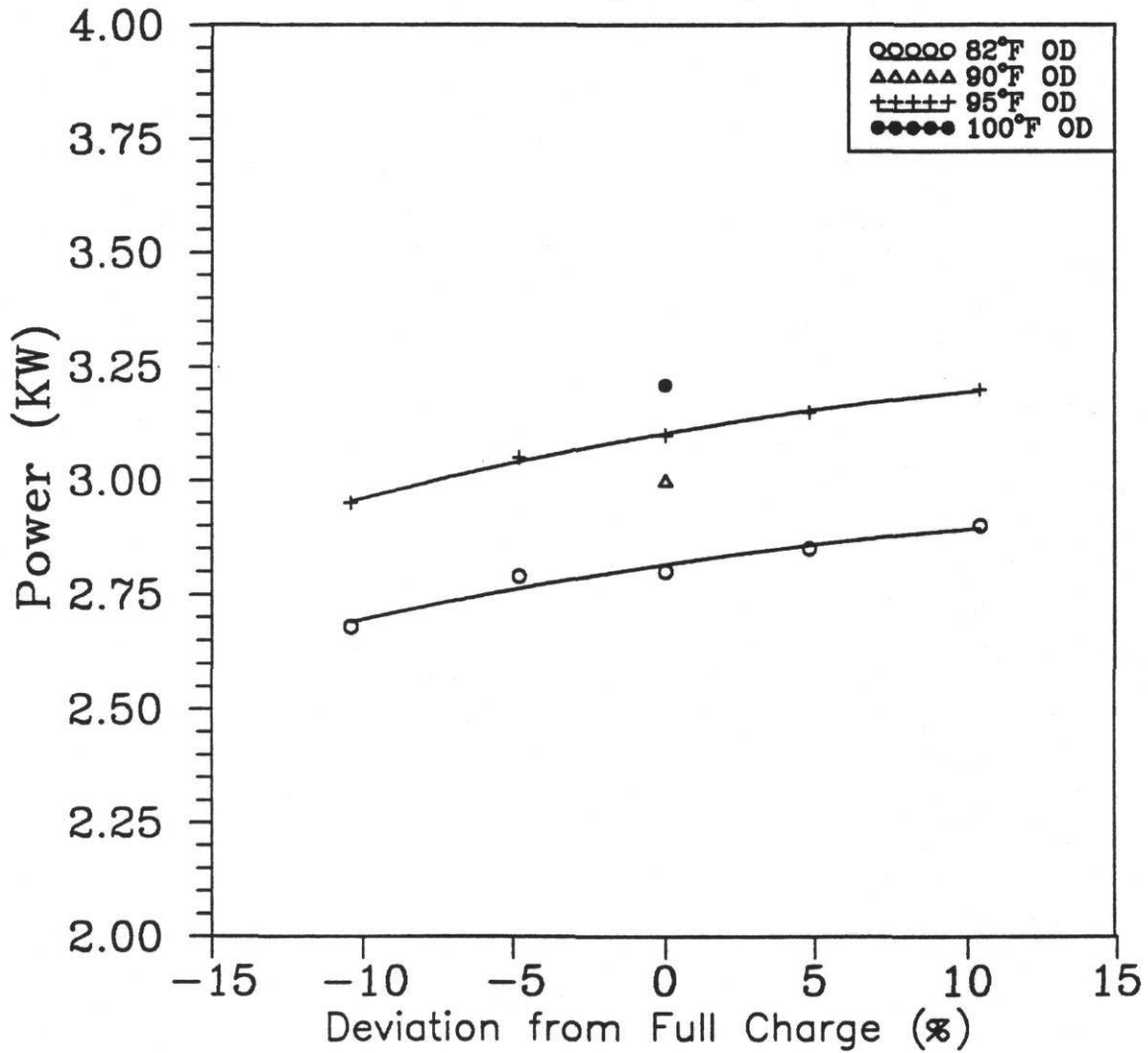


Figure 4.2 - Power consumption with the 0.075 inch diameter orifice.

Total Capacity as a Function of
Temperature and Charge
orifice (0.067)

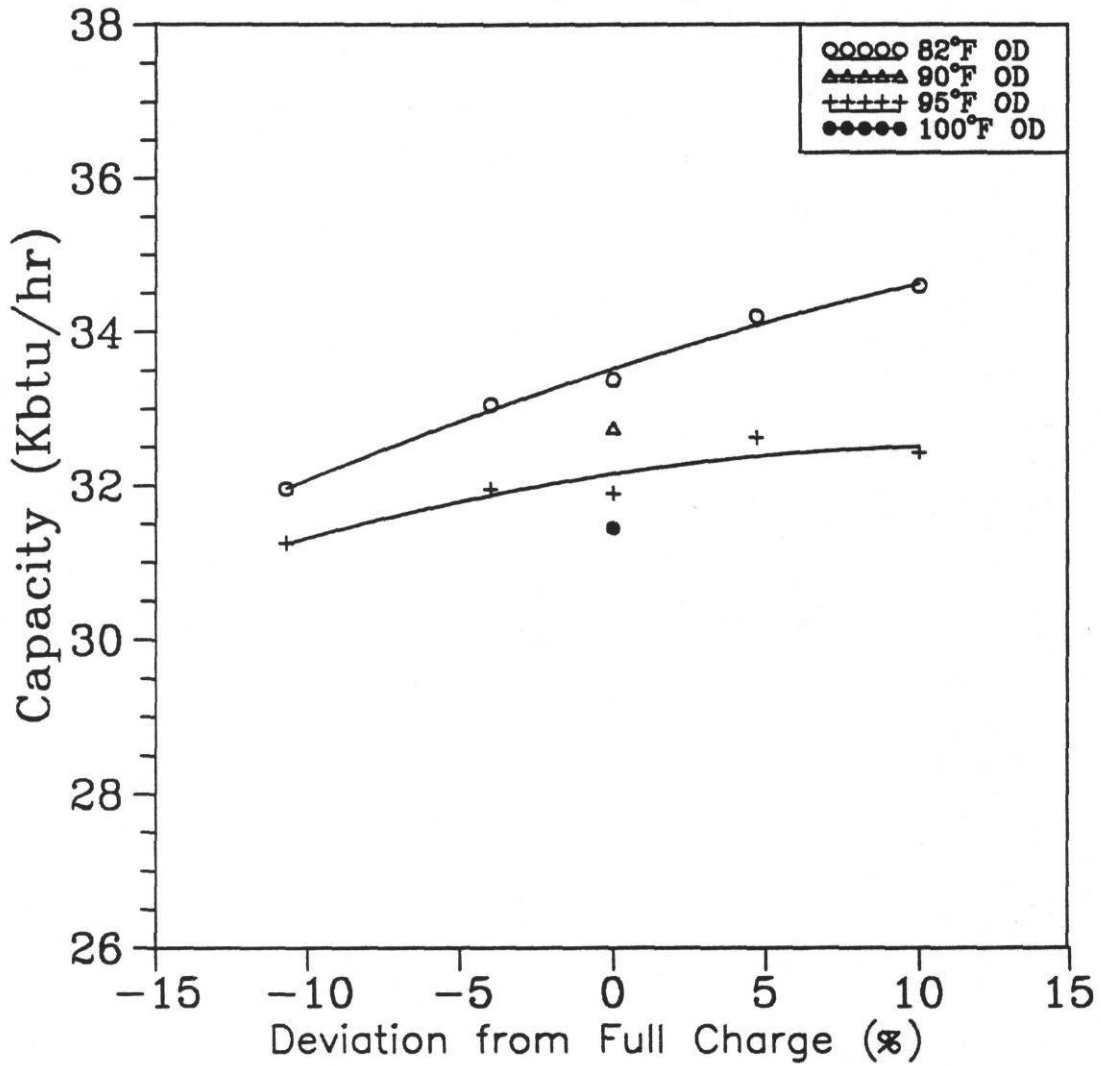


Figure 4.3 - Cooling capacity with the 0.067 inch diameter orifice.

Total Capacity as a Function of
Temperature and Charge
orifice (0.075)

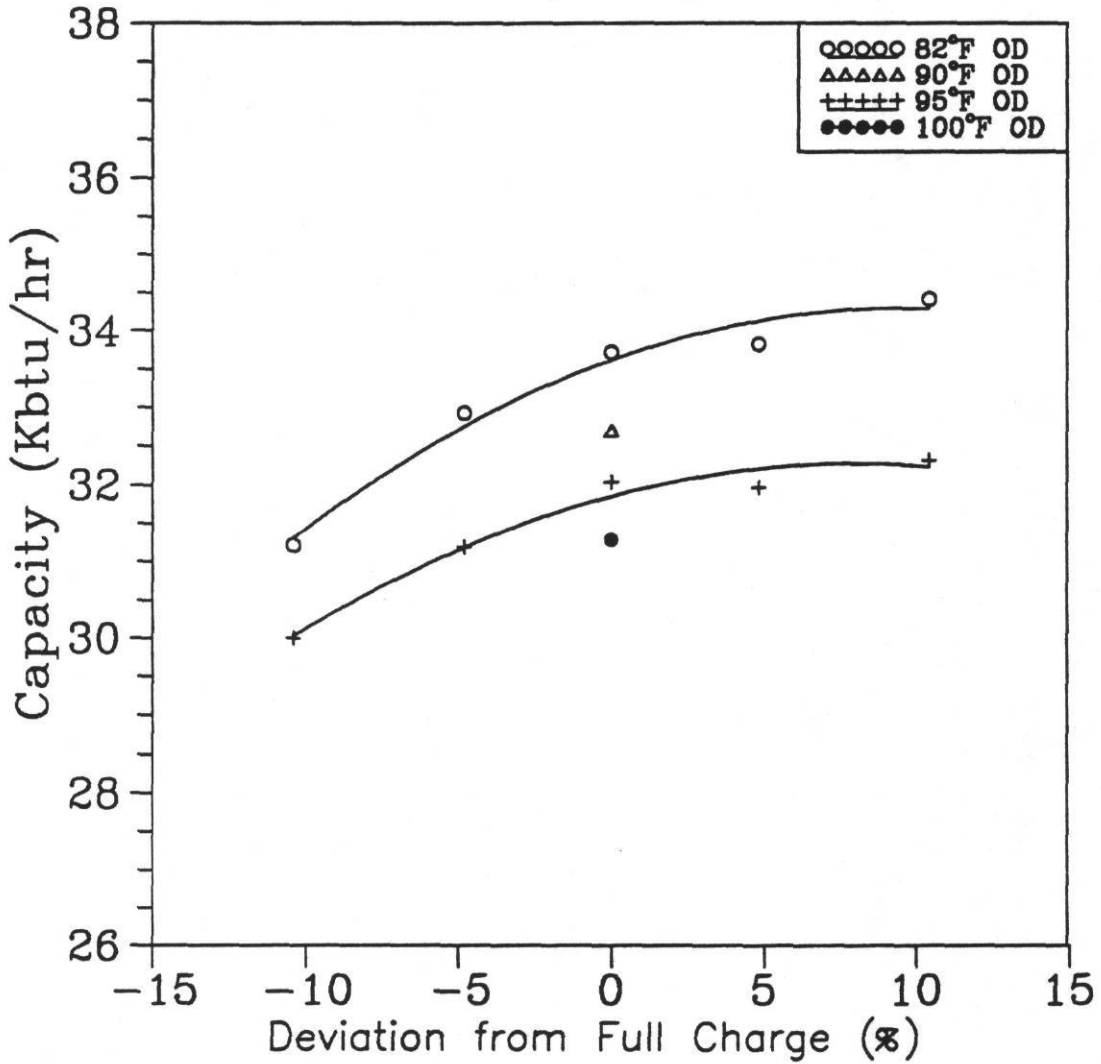


Figure 4.4 - Cooling capacity with the 0.075 inch diameter orifice.

Energy Efficiency Ratio as a Function of Temperature and Charge orifice (0.067)

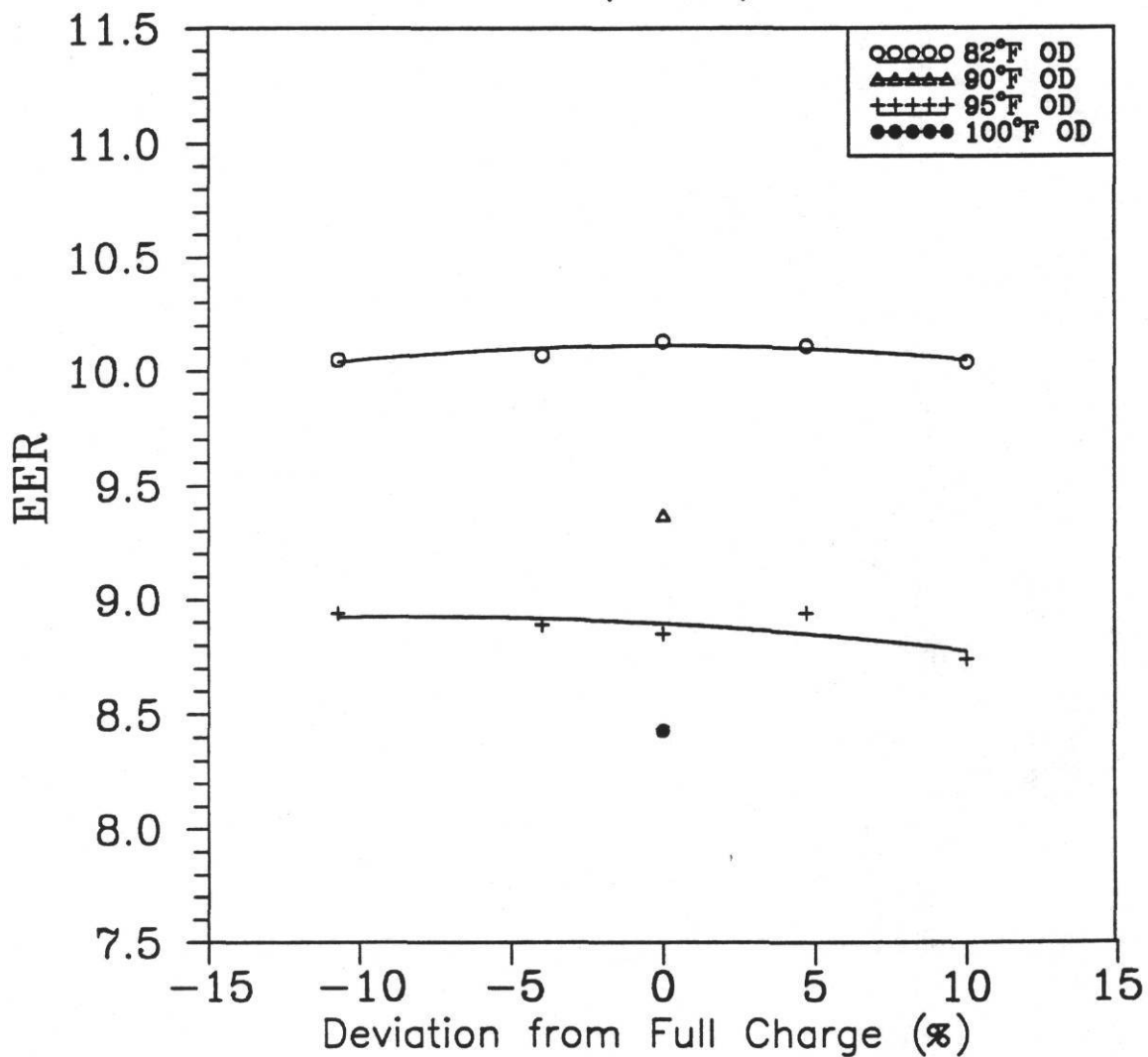


Figure 4.5 - Energy efficiency ratio with the 0.067 inch diameter orifice.

Energy Efficiency Ratio as a Function
of Temperature and Charge
orifice (0.075)

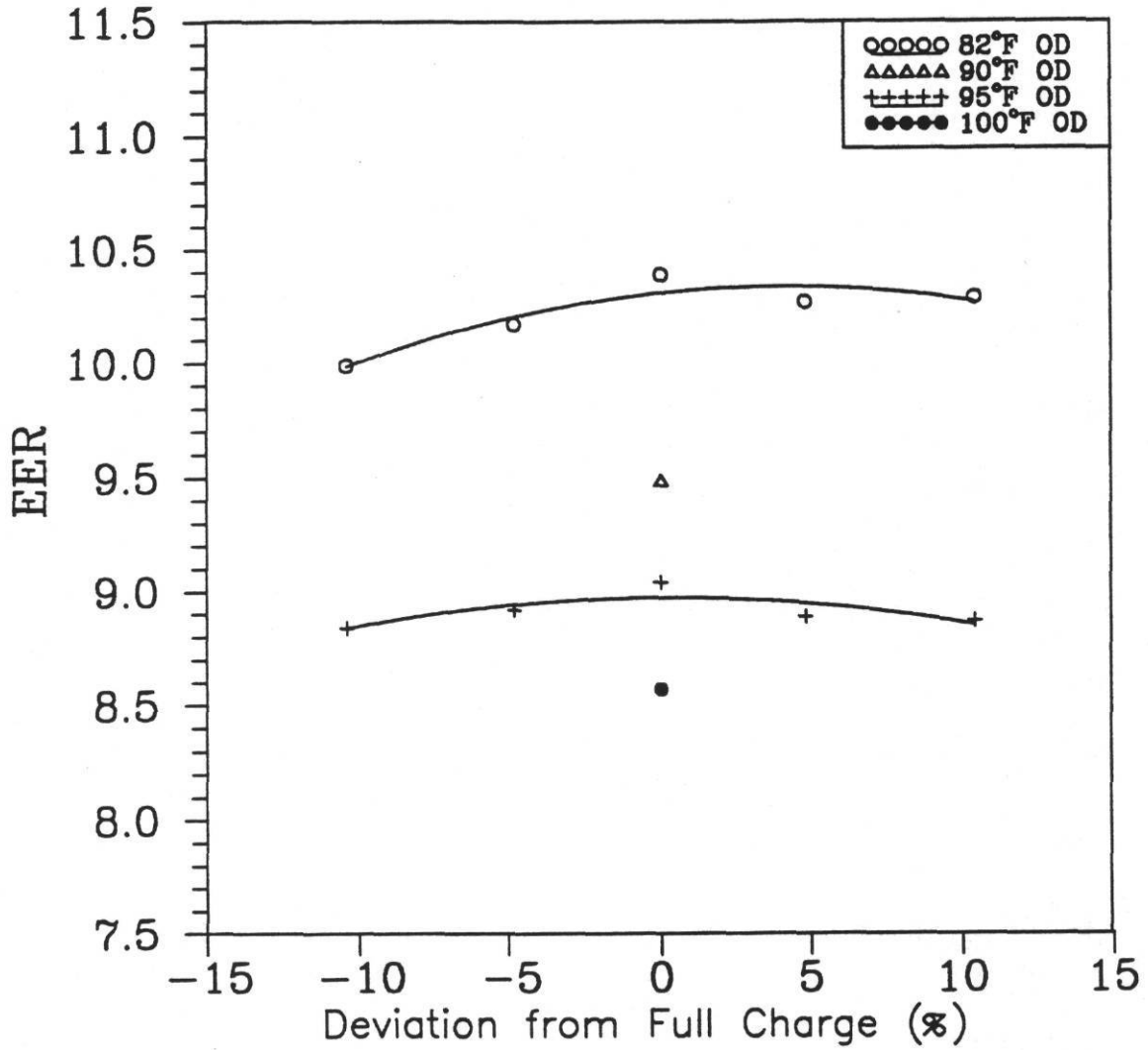


Figure 4.6 - Energy efficiency ratio with the 0.075 inch diameter orifice.

Superheat Temperature as a Function of Temperature and Charge orifice (0.067)

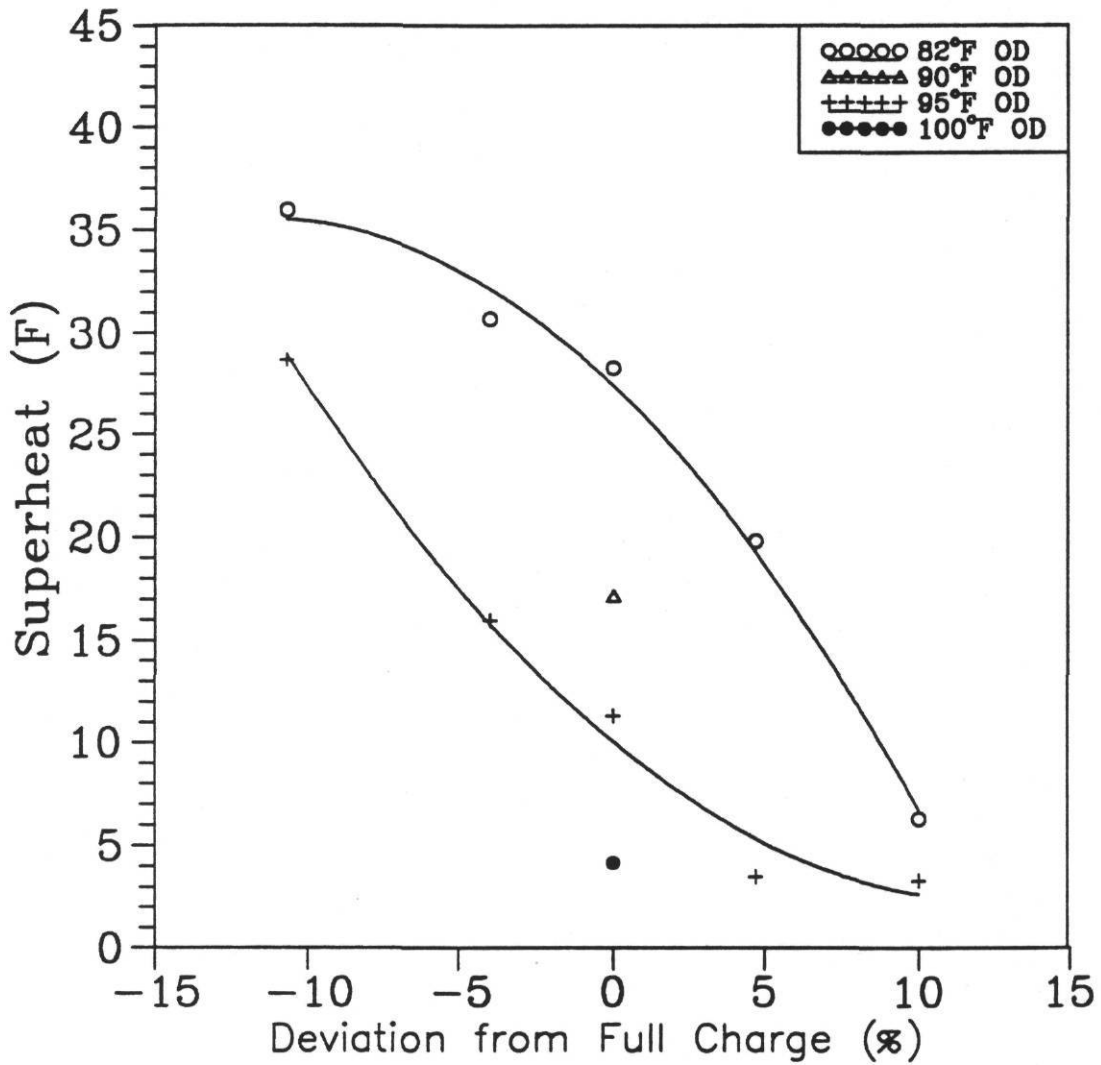


Figure 4.7 - Superheat near the quick disconnect with the 0.067 inch diameter orifice.

Superheat Temperature as a Function of Temperature and Charge orifice (0.075)

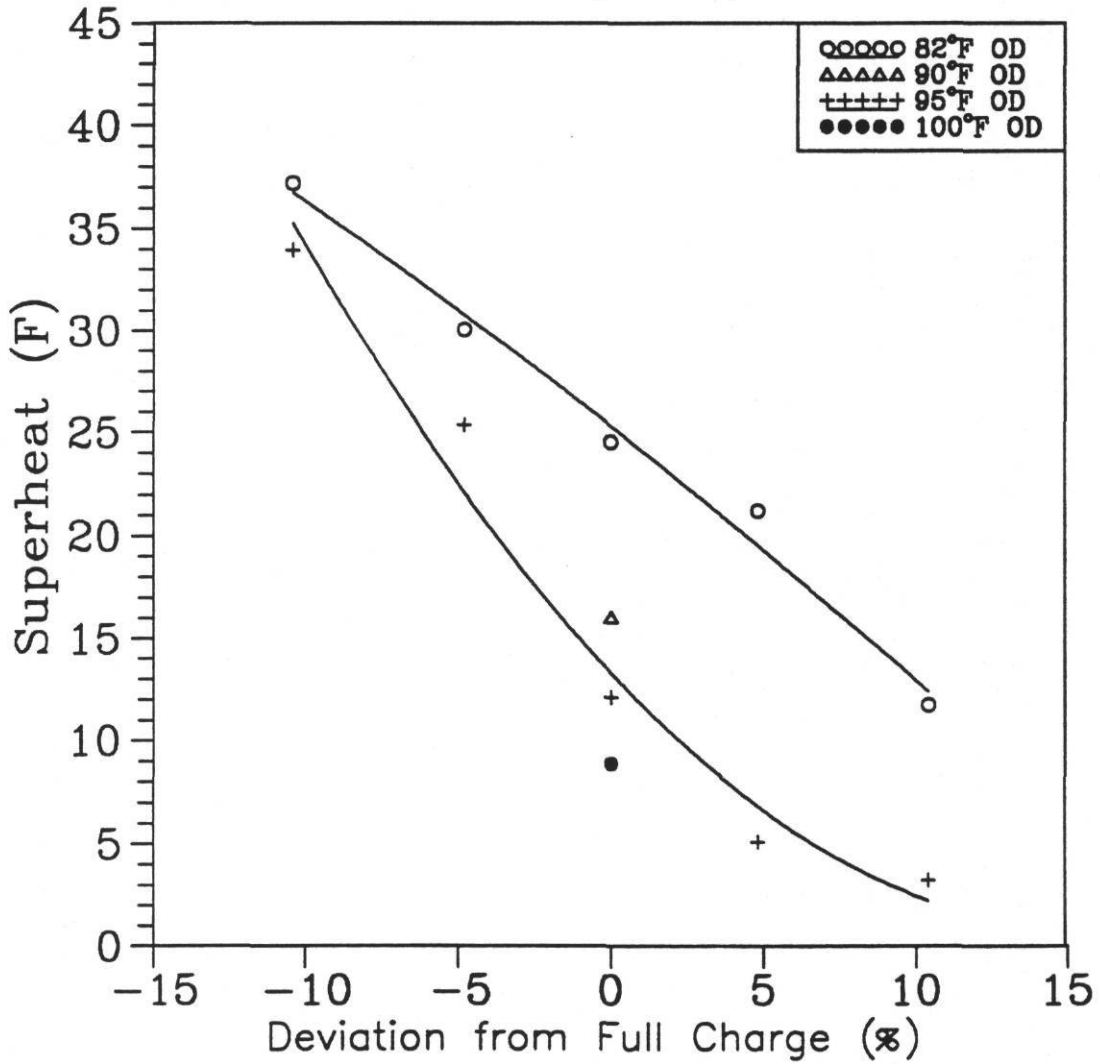


Figure 4.8 - Superheat near the quick disconnect with the 0.075 inch diameter orifice.

Subcooled Temperature as a Function of Temperature and Charge orifice (0.067)

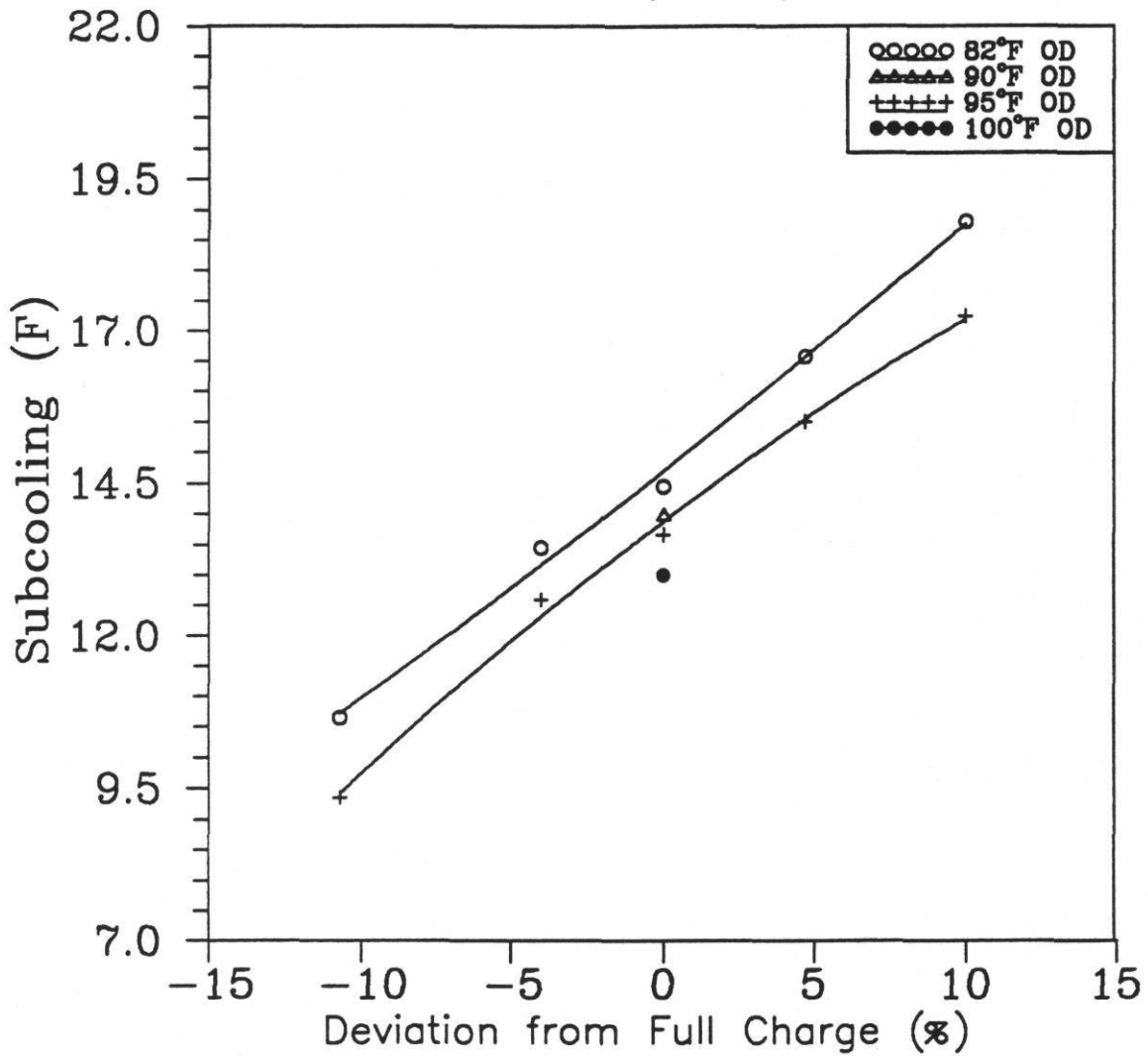


Figure 4.9 - Subcooling at the orifice inlet with the 0.067 inch diameter orifice.

Subcooled Temperature as a Function
of Temperature and Charge
orifice (0.075)

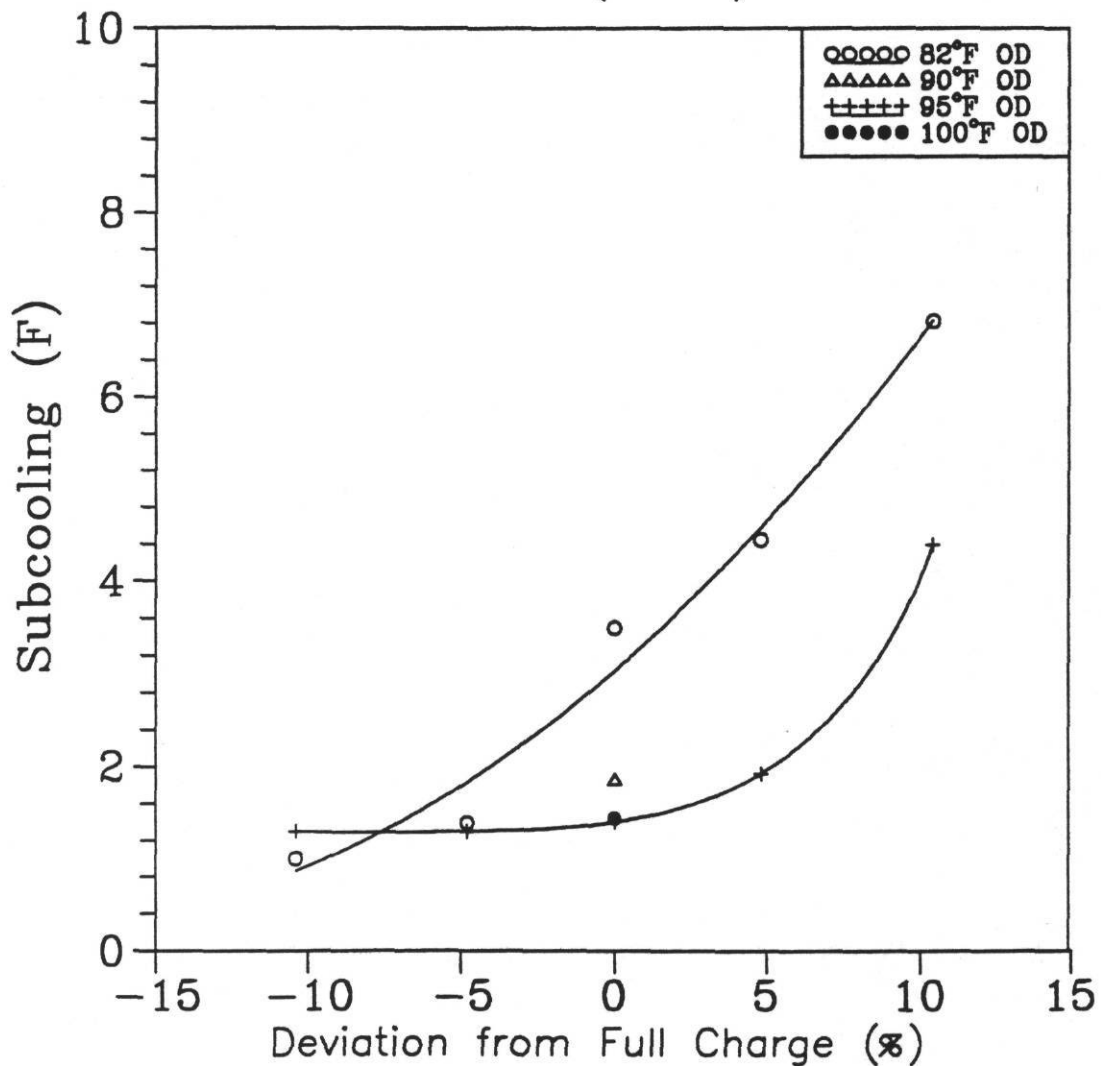


Figure 4.10 - Subcooling at the orifice inlet for the 0.075 inch diameter orifice.

the 0.067 inch diameter orifice compared to 232 psia with the 0.075 inch diameter orifice. The lower pressure at the orifice inlet would correspond to a lower condensing pressure. A lower condensing pressure would imply a larger enthalpy of condensation (vaporization). Thus, for the larger orifice, more of the heat transferred out of the refrigerant in the condenser was used in condensing the refrigerant rather than in producing subcooling as compared to the smaller orifice.

Figures 4.11 and 4.12 show the flow rates for the two orifices. The flowrates for the two orifices showed little variation. For the range of temperatures and charges investigated here, the flowrates were within 4%.

Refrigerant Flow Rate as a Function
of Orifice Inlet Pressure
orifice (0.067)

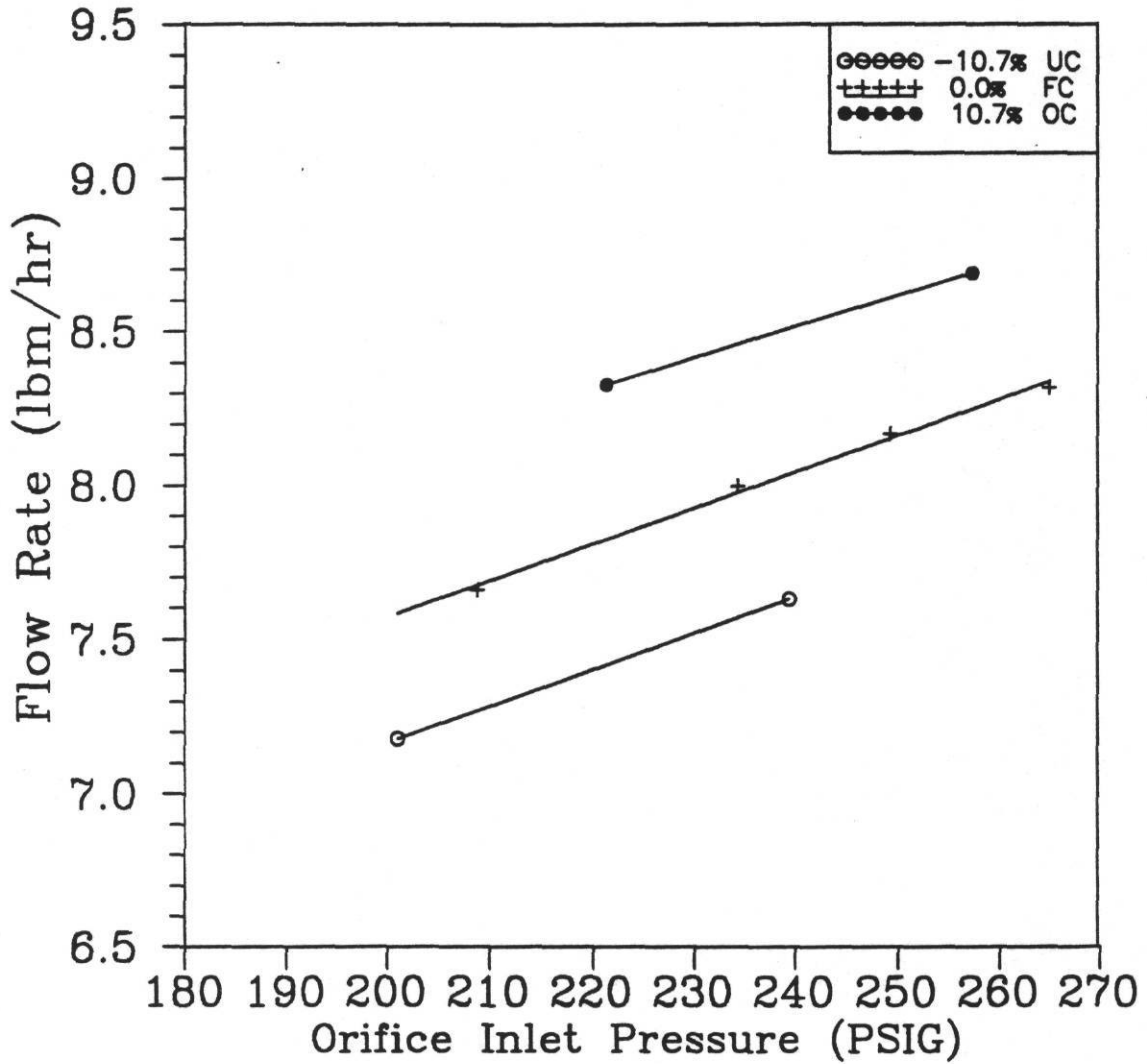


Figure 4.11 - Refrigerant flow rate with the 0.067
inch diameter orifice.

Refrigerant Flow Rate as a Function
of Orifice Inlet Pressure
orifice (0.075)

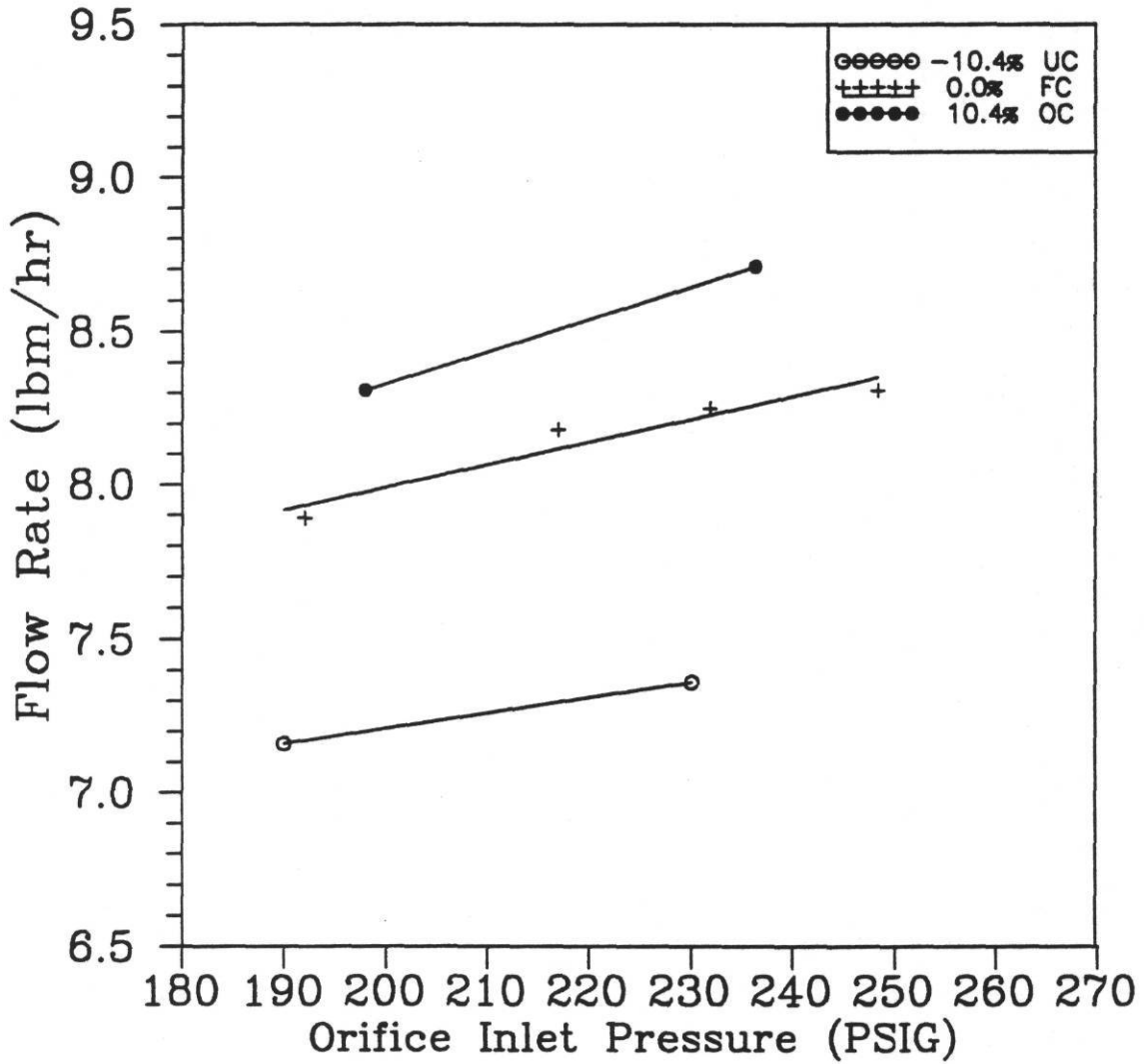


Figure 4.12 - Refrigerant flow rate with the 0.075 inch diameter orifice.

CHAPTER 5

COMPARISON OF THREE ORIFICES

The purpose of this chapter is to compare the overall system performance trends on some of the data collected for the three orifices. All results are presented for full charge. Recall that the amount of refrigerant for full charge in the three systems was 150, 136, and 125 ounces for the 0.067, 0.071, and 0.075 inch diameter orifices, respectively.

Figure 5.1 presents the total cooling capacity of the air conditioner for the three orifices for outdoor temperatures ranging from 82 to 95 F for full charge. The air conditioner showed the same trend of decreasing capacity with increasing outdoor temperature for all three orifices. The differences in capacity for the system with the three orifices was less than 500 Btu/hr at any of the temperatures tested. With the exception at 90 F, the nominal sized (0.071 inch) orifice produced the largest capacity with this air conditioning system.

Steady state EER results with outdoor temperature were similar to those of capacity (Figure 5.2). The system EER decreased with increasing temperature. In addition, the system EER for any of the orifices was within 0.3 Btu/wh at any of the temperatures. The 0.075 inch orifice had the highest EER for the three orifices at every temperature with the exception of 100 F.

The 0.075 inch orifice had the largest SEER for the three orifices even though it was only 0.3 points higher than the 0.067 orifice which had the lowest SEER (Table 5.1). The degradation coefficient, C_d , was largest for the nominal orifice and smallest for the 0.075 inch orifice.

Table 5.1 - SEER and C_d for three orifice sizes and full refrigerant charge.

Orifice Diameter (in)	SEER	C_d
0.067	9.5	0.116
0.071	9.6	0.130
0.075	9.8	0.112

Total Capacity at Full Charge as a Function of Outdoor Temperature and Orifices

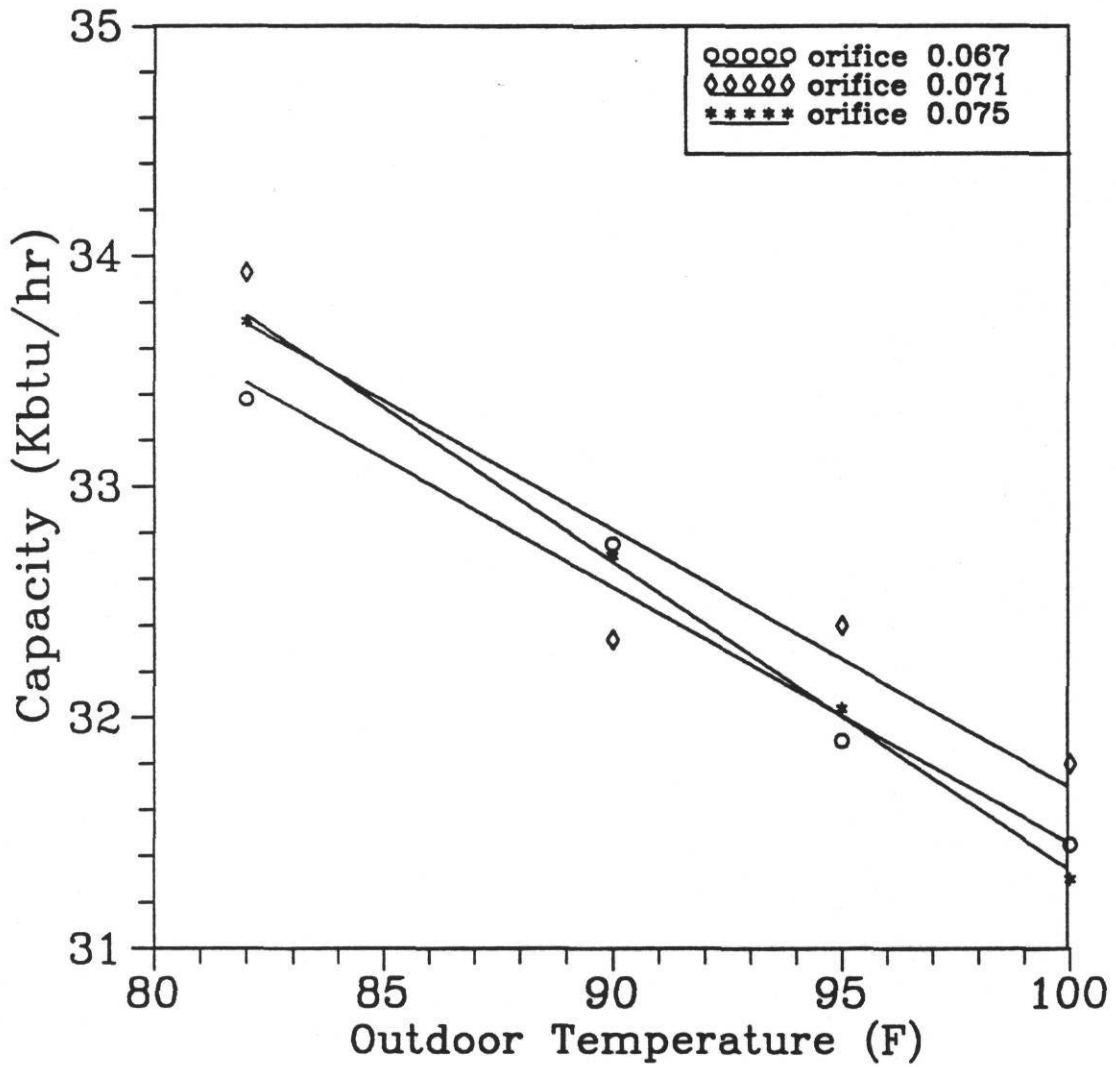


Figure 5.1 - Cooling capacity at full charge with the three orifices.

Energy Efficiency Ratio at Full Charge as a Function of Outdoor Temperature and Orifices

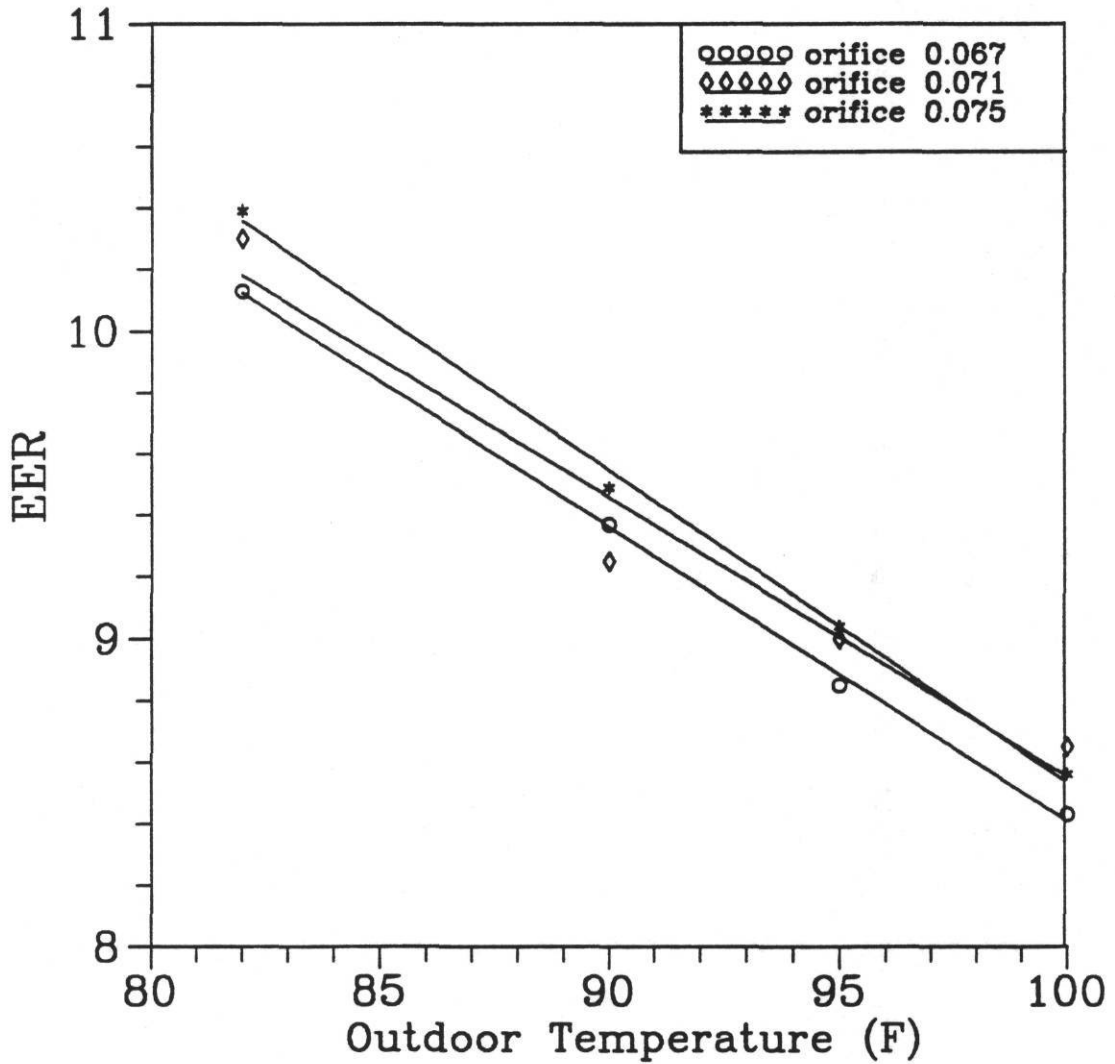


Figure 5.2 - Steady state energy efficiency ratio at full charge with the three orifices.

CHAPTER 6

CONCLUSIONS

This study was limited to measuring the performance of one residential sized central air conditioner. A limited number of tests were performed. Three different sized orifices were studied. The refrigerant charge was varied in the system from as much as 20% undercharging to 20% overcharging for the nominal orifice. Steady state measurements were made at outdoor temperatures ranging from 82 F to 100 F. Cycling tests were also performed to estimate the SEER of the unit.

One surprising result from this study is the small variation of EER and SEER to refrigerant charge. The results from earlier studies on capillary tubes suggested that a fixed expansion device would be extremely sensitive to changes in refrigerant charge. This result would seem to have important implications for the service technician in the field. It would be possible that he could miss the "rated" charge by perhaps as much as 10% (13 to 15 ounces in the system tested here) and see less than a 3% degradation in efficiency of the unit. For the capillary tube system tested earlier, this large of an over/under charge would produce an unacceptably large (7 to 10%) reduction in SEER.

The differences in behavior of the capillary and the orifices observed in this study have not been explained in the open literature. There has been a large number of basic studies on capillary tubes which characterize their response to two phase refrigerant flow through them. However, the authors have not seen a similar number of published studies on orifices. The observed differences in behavior of the two devices would suggest a need to do some basic studies on the orifices to better characterize flow versus conditions upstream and downstream of the orifice. A better characterization of orifices could be useful in predicting the performance of systems which use orifices.

Another conclusion from this study relates to the orifice sizing. From results presented in the previous chapter, the capacity varied little between the different orifices. The 0.075 inch orifice produced a slightly larger SEER. Thus, it would be possible to use the 0.075 inch orifice to replace the nominal (0.071 inch) orifice. There would be little change in the capacity and a small improvement in SEER over the nominal orifice. However, because the nominal refrigerant charge with the 0.075 inch

orifice is only 125 ounces compared to 136 for the nominal orifice, there would be a savings of 11 ounces of refrigerant in the system. This design change could produce a substantial reduction in refrigerant charge required to initially charge systems in the factory.